Seasonal and Spatial Changes in Gelatinous Zooplankton Trophic Roles in a Coastal Upwelling System

by

Elizabeth Ling-Na Rudy Wallace

A thesis accepted and approved in partial fulfillment of the

requirements for the degree of

Master of Science

in Biology

Thesis Committee:

Kelly Sutherland, Chair

Aaron Galloway, Member

Lucas Silva, Member

University of Oregon

Spring 2025

© 2025 Elizabeth Ling-Na Rudy Wallace

THESIS ABSTRACT

Elizabeth Ling-Na Rudy Wallace

Master of Science in Biology

Title: Seasonal and Spatial Changes in Gelatinous Zooplankton Trophic Roles in a Coastal Upwelling System

Gelatinous zooplankton are abundant throughout marine ecosystems, yet their trophic diversity is underappreciated. In the Northern California Current, gelatinous taxa including hydromedusae, ctenophores, siphonophores, chaetognaths, and pelagic tunicates, exist in a seasonally dynamic and highly productive eastern boundary current upwelling system. We analyzed carbon and nitrogen stable isotope composition ($\delta^{13}C$ and $\delta^{15}N$) of 539 gelatinous zooplankton samples of 36 species collected in winter and summer across shelf and offshore regions off the coast of Oregon and Washington, USA. Gelatinous zooplankton occupied many trophic roles, with $\delta^{13}C$ ranging from -24.04‰ to -14.85‰ and $\delta^{15}N$ ranging from 2.76‰ to 16.20‰, spanning approximately 4-7 trophic levels. During the summer upwelling season, gelatinous species had smaller isotope ranges individually and overall, with more differences between species compared to winter. In the winter, gelatinous species had larger isotope ranges with fewer differences between species, and the presence of low trophic level suspension feeders changed the overall gelatinous trophic space. Additionally, seven feeding mode groups of gelatinous zooplankton had distinct isotope values, supporting trait-based trophic roles. Understanding the trophic diversity of gelatinous zooplankton is essential for refining our knowledge of marine food webs and incorporating these taxa into ecosystem models.

ACKNOWLEDGMENTS

I would like to thank my advisor, Dr. Kelly Sutherland, for her guidance throughout this project, as well as my committee members, Dr. Aaron Galloway and Dr. Lucas Silva, for their feedback and advice. This project would not have been possible without the members of the Plankton Ecology Lab at Oregon State University, led by Dr. Su Sponaugle and Dr. Robert Cowen, and the Bluewater Lab at Portland State University, led by Dr. Anne Thompson, as well as the captains and crews of *R/V Sikuliaq*, *R/V Langseth*, and *R/V Sally Ride*, without whom no samples would have been collected. I would also like to thank the SPA Lab and Aoki Lab for allowing me to use their lab spaces and equipment, and I am especially grateful to Emily Huckstead for sharing her expertise in sample preparation and for so generously welcoming me into the SPA Lab.

For support throughout my degree, I would like to thank the staff of the Biology Department, IE^2, and OIMB, as well as my fellow graduate students for answering so many questions. I am grateful to my lab mates, Dr. Terra Hiebert, Dr. Alejandro Damian-Serrano, Farzana Yesmin, Audrey Lillie, Sophie Bagoye, Elaina Berdyck, and Will Bird for the community we created. I would like to thank Dr. Jess Lueders-Dumont for teaching me about stable isotopes and how to be a scientist, as well as my friends and family for their encouragement. Finally, I would like to thank my dog Moca for his continuous reminders to appreciate the world we live in.

This work was funded by a grant from the National Science Foundation, OCE-2125408, to Dr. Robert Cowen, Dr. Su Sponaugle, and Dr. Kelly Sutherland, also by generous contribution from Dr. Silva's laboratory funds, as well as by the Biology Department's William R. Sistrom Scholarship. Lastly, I would like to acknowledge the 17,000 planktonic animals included in this project.

TABLE OF CONTENTS

Chapter Page

I. SEASONAL AND SPATIAL CHANGES IN GELATINOUS ZOOPLANKTON TROPHIC ROLES IN A COASTAL UPWELLING SYSTEM 7

Introduction 7

Methods 9

Results 13

Discussion 23

Conclusion 33

APPENDIX: Supplementary methods, tables, and figures 33

REFERENCES CITED 39

LIST OF FIGURES

Figure Page

1. Environmental conditions in the sampling area 14

2. Crossplot of $\delta^{13}C$ and $\delta^{15}N$ values of all gelatinous zooplankton and larval fish samples separted by season and region 15

3. Crossplot of $\delta^{13}C$ and $\delta^{15}N$ values of all gelatinous zooplankton and larval fish samples separated by taxon 17

4. Seasonal shifts in resource use by gelatinous zooplankton species 21

5. Resource use by feeding mode 22

6. Scatter of co-occurrence ratio of species pairs vs. the pseudo-f-values of species pairs 26

CHAPTER I

SEASONAL AND SPATIAL CHANGES IN GELATINOUS ZOOPLANKTON TROPHIC ROLES IN A COASTAL UPWELLING SYSTEM

Introduction

Gelatinous zooplankton are abundant in many marine environments, and their importance as both predators and prey in marine food webs is increasingly being understood (Choy et al., 2017; Hays et al., 2018). This growing understanding of the role of gelatinous zooplankton in food webs necessitates deeper examination of the food web structure of these communities. Gelatinous zooplankton are often omitted from food web models or grouped into one category due to the belief that they are unimportant in food webs (Pauly et al., 2008). This belief is based on the high water content and low carbon content of gelatinous tissues and the scarcity of identifiable gelatinous taxa in the gut contents of predators (Lucas et al., 2011). However, recent methods developments have increasingly revealed trophic links involving gelatinous taxa (ex. Choy et al., 2017; Cavallo et al., 2018; Hetherington et al., 2019; Dischereit et al., 2024), motivating further examination of the diverse roles of gelatinous organisms in marine food webs.

Despite the common characteristic of high water and low carbon content, gelatinous zooplankton belong to multiple phyla and have diverse body plans, life histories, and feeding methods. This group includes scyphomedusae “true jellyfish” as well as hydromedusae, siphonophores, ctenophore comb jellies, pelagic tunicates, chaetognath worms, and some pelagic polychaete worms. Not only do different gelatinous taxa have distinct roles in food webs, but they may respond in unique ways to changes in their environment. The dynamics of gelatinous zooplankton food webs across temporal and environmental gradients have not yet been explored.

Food web structure dictates the transfers of matter and energy through ecosystems, and understanding food webs is essential for conservation and management (Pace et al., 1999). Marine food web theory is based on fish following gape limitation and the optimal foraging theory which conclude that fish will eat the largest prey that fits in their mouth because it is the most efficient (Lindeman, 1942; Elton, 1927). This underlies the theory that in marine systems, higher productivity leads to larger phytoplankton and increased omnivory, which in turn leads to shorter food chains overall (Ryther et al., 1969; Miller et al., 2010; Lerner et al., 2022).

Gelatinous zooplankton diverge from these principles because they have different feeding mechanics including passive prey capture with tentacles, entraining prey in a feeding current, and filter feeding, in addition to active ambush and hunting (ex. Haddock, 2007; Kiørboe, 2011; Conley et al., 2018; Corrales-Ugalde & Sutherland, 2021). These feeding mechanics select prey based on factors such as fluid mechanics (Corrales-Ugalde & Sutherland, 2021) and nematocyst/tentilla morphology (Damian-Serrano et al., 2021) and do not follow gape limitation nor allow for omnivory in the same way as fish. Thus, we would not expect gelatinous taxa to follow the same trophic dynamics as fish across environmental gradients.

Diets of gelatinous zooplankton have been examined though feeding observations and visual and molecular gut contents analysis, which provide detailed snapshots of what organisms have recently consumed (ex. Choy et al., 2017; Corrales-Ugalde et al., 2021; Damian-Serrano et al., 2022; Hiebert et al., 2025, Masterman et al., in review). For a time-integrated, broad scale perspective of a whole ecosystem, stable isotope analysis can be used.

In animal tissues, nitrogen stable isotope composition ($\delta^{15}N$) indicates the animal's trophic level, while carbon ($\delta^{13}C$) indicates carbon source (DeNiro & Epstein, 1978; Minagawa & Wada, 1984; Peterson & Fry, 1987; Post, 2002). $\delta^{13}C$ and $\delta^{15}N$ stable isotope analysis has been used to examine gelatinous zooplankton in a few studies which have found a wide range of trophic levels and have investigated population connectivity (Chi et al., 2021; Hetherington et al., 2024). In the tropical east Atlantic, gelatinous zooplankton covered a range of over three trophic levels, and some taxa had distinct isotopic compositions in shallow vs. deep water while others did not (Chi et al., 2021). In the southern California Current, siphonophores alone spanned 1.5 trophic levels, as determined through stable isotope analysis (Hetherington et al., 2024). Seasonal variability in gelatinous zooplankton trophic roles has not yet been explored using stable isotope analysis.

Variations in gelatinous food web structure across different seasons and environments can be best examined in an area that provides a patchwork of environmental conditions, such as the Northern California Current (NCC). The NCC is an eastern boundary current with seasonal upwelling located in the northeast Pacific. It experiences pulses of strong wind-driven upwelling in the summer months which fuel high productivity on the continental shelf, while in the winter months downwelling often prevails (Peterson et al., 1979; Huyer, 1983; Hickey & Banas 2003). In this exploratory study, our goal was to examine the trophic structure of the gelatinous

zooplankton food web in the NCC in both summer and winter. Due to the variety of diets and feeding modes in this group, we expected that the gelatinous species and feeding mode groups would occupy distinct trophic niches and the trophic space occupied by gelatinous organisms overall would be large. This study gives broad-scale insight into the diversity of roles gelatinous zooplankton occupy in marine food webs and the ways gelatinous food webs respond to changing environmental conditions.

Methods

Sample collection

In 2022 – 2023, we collected gelatinous zooplankton samples aboard four research cruises in the Northern California Current (NCC) off the coast of Oregon and Washington, USA. Two sampling trips occurred in the winter during the "downwelling" phase of the NCC (March 1-12, 2022, *R/V Sikuliaq* SKQ202204S, and February 16-March 1, 2023, *R/V Sikuliaq* SKQ202303S), while the remaining two cruises took place in summer during the "upwelling" phase (July 18-30, 2022, *R/V Langseth* MGL2207 and August 9-21, 2023, *R/V Sally Ride* SR2317). During each of the winter 2022 and summer 2023 cruises we collected samples at 28 stations along four 80km latitudinal transects and two 160km latitudinal transects encompassing the shelf, slope, and offshore regions (Figure 1A). Due to rough weather during the winter 2023 cruise, 20 stations were sampled, and during the summer 2022 cruise 26 stations were sampled. There were 102 sampling events across all four cruises. This sampling scheme facilitated comparisons across environmental gradients by encompassing the extremes of temperature and nutrient supply that affect this region.

We collected samples using a Multiple-Opening-Closing-Net-Sampling-System (MOCNESS) system deployed during daylight hours. Samples for this project came from the surface depth increment, usually 0-25m, and were collected in the net with $1m^2$ area and 333µm mesh size. At each station, a Conductivity-Temperature-Depth sensor package (CTD) was also deployed to collect salinity, temperature, fluorescence, and oxygen profiles. Upon retrieval of the MOCNESS, we picked gelatinous zooplankton and larval fish samples from a chilled backlit tray and grouped them by lowest visually identifiable taxon (genus or species-level). Each grouped sample was placed in a Whirlpak with minimal extra seawater to limit additional salt that would

affect the mass of dried samples. Samples were stored at -80°C aboard the ship and -20°C upon return to land.

Sample processing

We analyzed gelatinous zooplankton and larval fish samples for nitrogen and carbon stable isotope composition, reported as $\delta^{15}N$ vs. air standard and $\delta^{13}C$ vs. VPDB standard, as well as %C and %N by mass. To prepare samples, each sample was thawed at room temperature and transferred to an aluminum weigh boat. We measured wet weight of each sample using an analytical balance to the nearest 0.01mg. The sample was then dried at 60°C for five days, the length of time found to be required for all species to achieve complete desiccation such that they became dry powder when crushed. A few species had slightly different prep methods, see Appendix for explanation. Immediately after removal from the oven, dry weight was recorded to the nearest 0.01mg. Samples were then crushed to a fine powder and homogenized using an agate mortar and pestle. Up to 10 mg of each sample was weighed out to the nearest 0.001 mg and was packed in a tin capsule for analysis, with exact weights recorded for calculations. Based on %C and %N estimates from literature review and a preliminary batch of samples, for which all samples were ~4 mg, sample weights were varied to keep the amount of C and N in each sample roughly consistent across all samples regardless of taxon. For example, fish larvae and chaetognaths with estimated %C=40 and %N=10 were prepared with much lower sample masses than hydromedusae with %C and %N <5.

Samples were measured for $\delta^{13}C$, $\delta^{15}N$ %C, and %N on an Elemental-Analyzer Isotope Ratio Mass Spectrometer (EA-IRMS) at the UC Davis Stable Isotope Facility. Multiple international and in-house standards were used to calibrate measurements.

Analytical precision (jelly standards)

Three of the gelatinous zooplankton samples were run as standards every ~12 samples throughout the measurement process. These samples were homogenized jellyfish tissue that was prepared in the same way as the other gelatinous zooplankton samples, so their analytical precision should approximate that which the other samples would have if replicates were run. Winter 2022 Grays Harbor transect station 1 *Aurelia labiata* had a $\delta^{13}C$ standard deviation of 0.170‰ and a $\delta^{15}N$ standard deviation of 0.299‰. (Means $\delta^{13}C$ =-17.56‰ and $\delta^{15}N$=10.51‰, n=24). Summer 2023 Grays Harbor transect station 6 *Aequorea victoria* had a $\delta^{13}C$ standard deviation of 0.1675‰ and a $\delta^{15}N$ standard deviation of 0.370‰ (means $\delta^{13}C$=-20.88‰ and

$\delta^{15}N$=11.72‰, n=14). Summer 2023 Grays Harbor transect station 1 *Aequorea victoria* had a $\delta^{13}C$ standard deviation of 0.169‰ and a $\delta^{15}N$ standard deviation of 0.457‰ (means $\delta^{13}C$=-17.27‰ and $\delta^{15}N$=11.35‰, n=14). The average standard deviations for these three standards are: 0.169‰ for $\delta^{13}C$ and 0.374‰ for $\delta^{15}N$.

Data analysis

To compare the summer and winter environmental conditions, daily Cumulative Upwelling Transport Index (CUTI) values (Jacox et al., 2018) were downloaded from https://mjacox.com/upwelling-indices/. We examined the daily CUTI for the duration of each cruise as well as 21 days prior to each cruise. We chose 21 days as the period of time that would have an influence on the gelatinous zooplankton stable isotope composition based on Spitz et al., (2005) observation that zooplankton abundances respond to environmental conditions in 13-16 days, as well as an approximate intermediate value of stable isotope half-life estimates in scyphozoans. Schaub et al., (2021) found a half-life of 15 days for $\delta^{13}C$ and a half-life of 36 days for $\delta^{15}N$ in *Chrysaora pacifica*, while D'Ambra et al., (2014) found a half life of 9-10 days for both isotopes in *Aurelia aurita*. Using twice the half-life as a rough estimate of the time required for tissues to reach steady state with the diet, (D'Ambra et al., 2014), steady state occurs in 30, 72, or 18-20 days following a shift in diet.

All $\delta^{13}C$ values were corrected for lipid content based on their C:N ratio according to Post et. al., (2007), as lipids are depleted in 13-C compared to proteins and carbohydrates, so samples with different amounts of lipids are not directly comparable. The equation used was:

$\delta^{13}C\text{-corrected} = \delta^{13}C - 3.32 + 0.99*(C:N \text{ by mass})$

Samples were separated into "shelf" and "offshore" regions based on the observation that in both summer and winter the chlorophyll fluorescence measurements increased where the seafloor depth was <~250m, indicating increased productivity. This isobath was used to separate samples by their collection location.

Data analysis was conducted in R version 4.3.2 (R Core Team, 2023). CTD data was analyzed using the oce package (v.1.8-2, Kelley & Richards, 2023). Visualizations were made using ggplot2 (v.3.5.0, Wickham, 2016). Permanovas were done by making Euclidian distance matrices using the "vegdist" function from the vegan package (v. 2.6-10, Okansen et al., 2025) followed by the "adonis2" function. Post-hoc multivariate pairwise comparisons were made using the "pairwise.perm.manova" function from the RVAideMemoire package (v.0.9-83-7,

Herve, 2023) with "fdr" method for multiple comparisons p-value adjustment. To compare univariate data (such as $\delta^{13}C$ or $\delta^{15}N$ only), the "pairwise.perm.t.test" function from the RVAideMemoire package with the "fdr" adjustment was used. Single univariate pairwise comparisons (such as between summer and winter $\delta^{13}C$) were done with a Welch's two-sample t-test using the "t.test" function from the stats package.

Stable isotope niche analysis

We used the SIBER package in R (Jackson et al., 2011) to calculate standard ellipses of each species in each season separated by shelf/offshore region, and each feeding mode group in each season. We focused on the Bayesian standard ellipses, which provided an estimate of the uncertainty due to sampling a subset of the population rather than the entire population. At small sample sizes the estimates can vary, while they converge on the population standard ellipse as n approaches infinity. 4000 40% standard ellipse estimates (containing ~40% of the data) were generated for each group. Each of these 4000 ellipses was represented by the x and y (mean $\delta^{13}C$ and mean $\delta^{15}N$) values of its center and its covariance matrix which included the variance of x and of y ($\delta^{13}C$ and $\delta^{15}N$) as well as the covariance of x and y.

We used these Bayesian standard ellipses to examine the difference in isotope values and ellipse areas between seasons (Figure 4). For each group, from these 4000 Bayesian ellipses we calculated the mean and the variance of the ellipse center $\delta^{13}C$ and $\delta^{15}N$ estimates and the mean and variance of the standard ellipse area estimates. For each species on the shelf and offshore we calculated the difference between the means of summer and winter for $\delta^{13}C$ and $\delta^{15}N$ by subtracting the mean of all the ellipse center estimates for winter from the mean for summer. The variance of this difference (standard deviation squared) is:

$$\text{var}(\delta^{13}C \text{ summer estimates}) + \text{var}(\delta^{13}C \text{ winter estimates}) - 2\text{cov}(\delta^{13}C \text{ summer estimates}, \delta^{13}C \text{ winter estimates})$$

(and the equivalent for $\delta^{15}N$). We then plotted summer-winter $\delta^{13}C$ vs. summer-winter $\delta^{15}N$ with the error bars as one standard deviation of the difference (the square root of the variance of the difference calculated above).

Similarly, to compare the differences between the summer and winter standard ellipse areas for each species, we calculated the difference of the mean of the 4000 Bayesian standard ellipse areas for each species/season group. We also calculated the variance of the 4000 ellipse area estimates for each species/season and calculated the covariance between the summer and

winter ellipse area estimates. This allowed us to calculate the variance of the difference of the mean standard ellipse areas as:

var(summer ellipse area)+var(winter ellipse area)-2cov(summer ellipse area, winter ellipse area)

We then plotted the difference of the mean Bayesian ellipse area for each species, with the error bar as the square root of the variance calculated above, or one standard deviation.

Results

Oceanographic setting

Oceanographic measurements revealed distinct environmental conditions between summer and winter as well as between the shelf and offshore regions. The sea surface temperature at 5m depth was highest offshore for all transects during all cruises, but especially during summer (Figure 1B). During the two winter cruises, offshore temperatures were slightly higher than temperatures near the coast (all temperatures within 8.07-10.14°C). During summer, the offshore temperatures reached 17.60°C in summer 2022 and 19.85°C in summer 2023, then dropped to <10°C near the coast, with a minimum of 7.64°C in summer 2022 and 9.97°C in summer 2023.

Surface fluorescence was relatively low far from the coast across both seasons (0.695 mg/m^3 average across all stations 4, 5, and 6), and in both seasons increased near the coast (Figure 1C). In the winter, fluorescence near the coast reached 1.88 mg/m^3 (average of station 1 on all winter transects) while in the summer fluorescence was highest at the first or second station from the coast, reaching 10.03 mg/m^3 (average of the highest surface fluorescence measurement on each summer transect). The highest surface fluorescence was during summer 2022 on the Newport Harbor line at station 2, 23.09 mg/m^3.

The daily CUTI upwelling index averaged within each latitude bin had a median of 0.44 in summer 2022 and 0.52 in summer 2023, but 0.14 in winter 2022 and 0.17 in winter 2023 (Figure 1D). The mean of the daily CUTI was significantly different between summer and winter cruises (pairwise t-tests, fdr p-value adjustment, $p<0.05$), but not between cruises of the same season in different years. In all four cruises, median CUTI values were above zero, indicating upwelling conditions in both the summer and winter months, but with upwelling about twice as strong in summer compared to winter (Figure 1D).

Overall, the summer shelf was characterized by surface temperatures 8-10°C, high fluorescence, and a high upwelling index. The summer offshore had surface temperatures 17-20°C and low fluorescence. The winter shelf had temperatures 8-10°C, slightly elevated surface fluorescence, and a low (but positive) upwelling index, and the winter offshore also had temperatures 8-10°C but with low fluorescence.

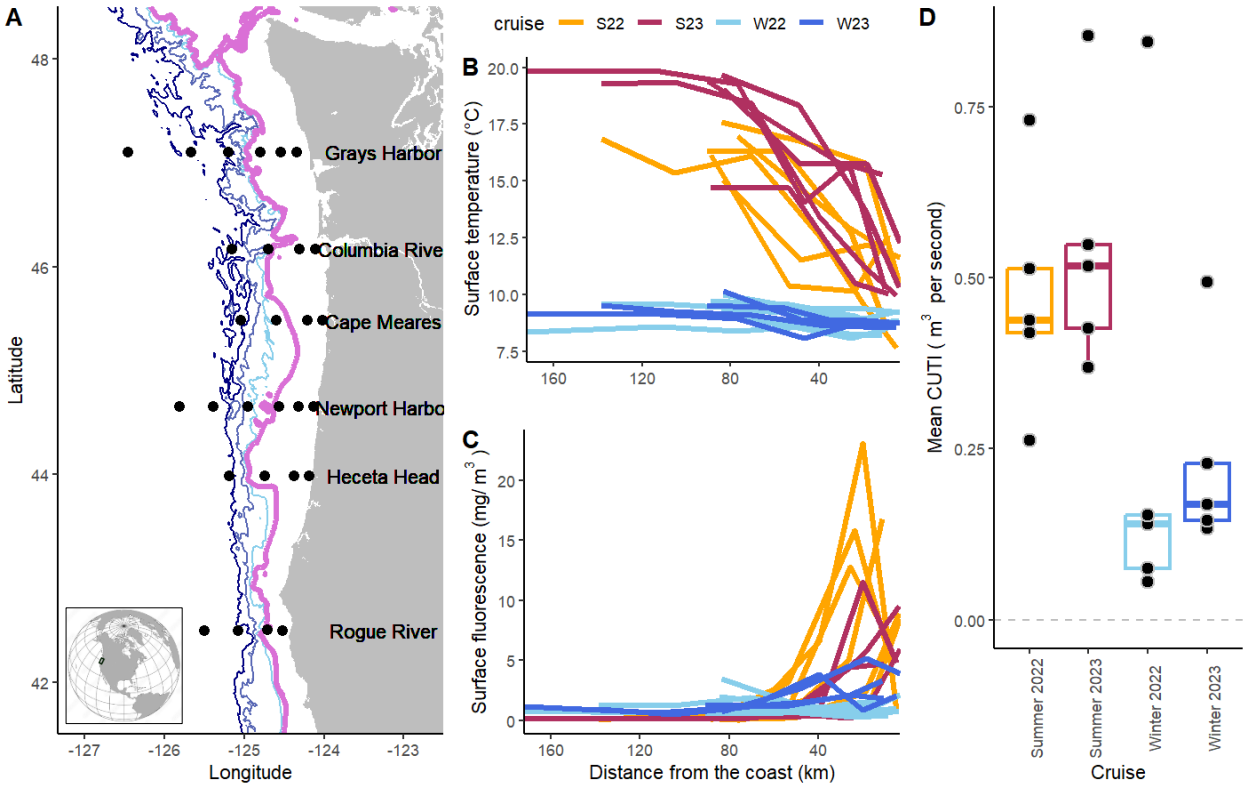


Figure 1. Environmental conditions in the sampling area: A) Map of sampling area with sampling locations along six transects marked with dots and bathymetry shown in contours (pink is 250m, blues light to dark are 500m, 1000m, 1500m). Bathymetry data is from GEBCO (GEBCO Compilation Group, 2024). Inset shows the sampling area on a global map. B) Water temperature (°C) at 5m depth vs. distance from the coast (km). C) Fluorescence (mg/m^3) at 5m depth vs. distance from the coast (km). For B) and C), colors indicate each cruise, and lines connect temperature measurements for each transect of each cruise. D) CUTI upwelling indices during each of the four cruises. The five dots are the means of daily indices during the sampling cruise and 21 days before the cruise, averaged within each of the five one-degree latitude bins of the sampling area (43°N though 47°N). Boxplots were created from these mean values.

All gelatinous zooplankton and larval fish $\delta^{13}C$ and $\delta^{15}N$

We analyzed 539 gelatinous zooplankton (and larval fish) samples, representing six phyla and 36 species: 137 from summer 2022, 148 from summer 2023, 102 from winter 2022, 146 from winter 2023, and 3 aggregated from multiple cruises. Overall, the 539 samples spanned a $\delta^{13}C$ range of 9.19‰ and a $\delta^{15}N$ range of 13.44‰ (Figure 2). The minimum and maximum $\delta^{13}C$ and $\delta^{15}N$ were all found in winter 2023. The $\delta^{13}C$ ranged from -24.04‰ (winter 2023 Columbia River transect station 3 *Clione limacina*) to -14.85‰ (winter 2023 Grays Harbor transect station 5 *Limacina helicina*), and the $\delta^{15}N$ ranged from 2.76‰ (winter 2023 Columbia River transect station 3 *Solmissus spp.*) to 16.20‰ (winter 2023 Newport Harbor transect station 6 *Beroe spp.*).

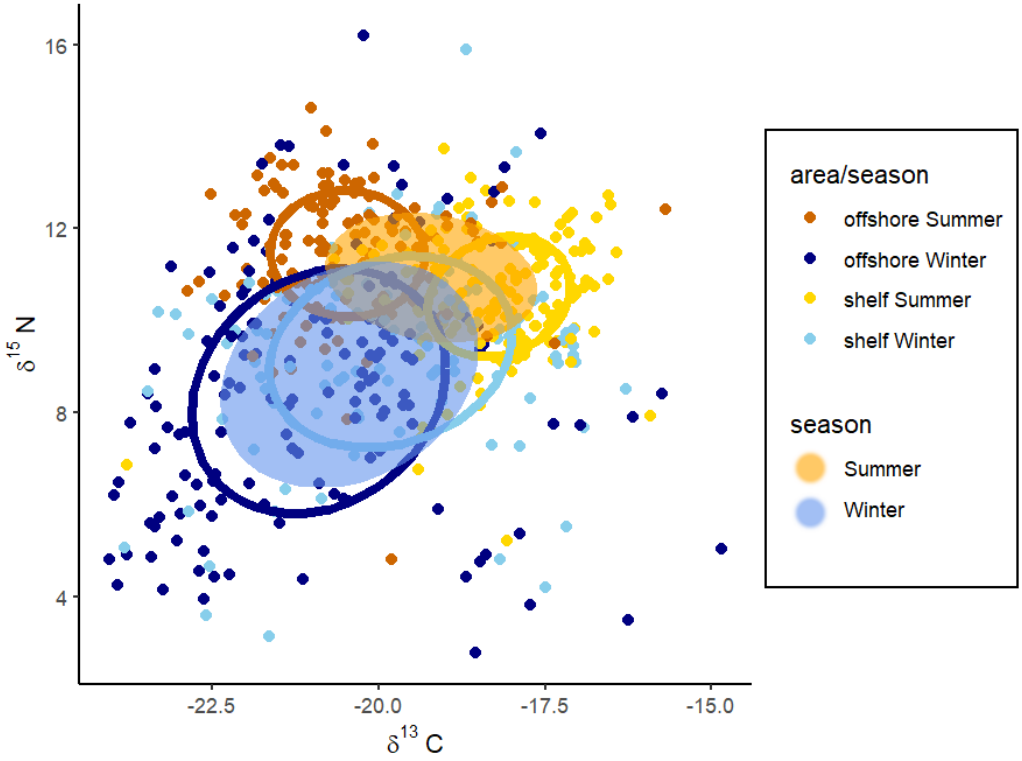


Figure 2: Crossplot of $\delta^{13}C$ and $\delta^{15}N$ values of all gelatinous zooplankton and larval fish samples separated by season and region. Filled ellipses are 40% ellipses for summer (orange) samples and winter (blue) samples. Solid outlines are 40% ellipses for four summer/winter and shelf/offshore categories.

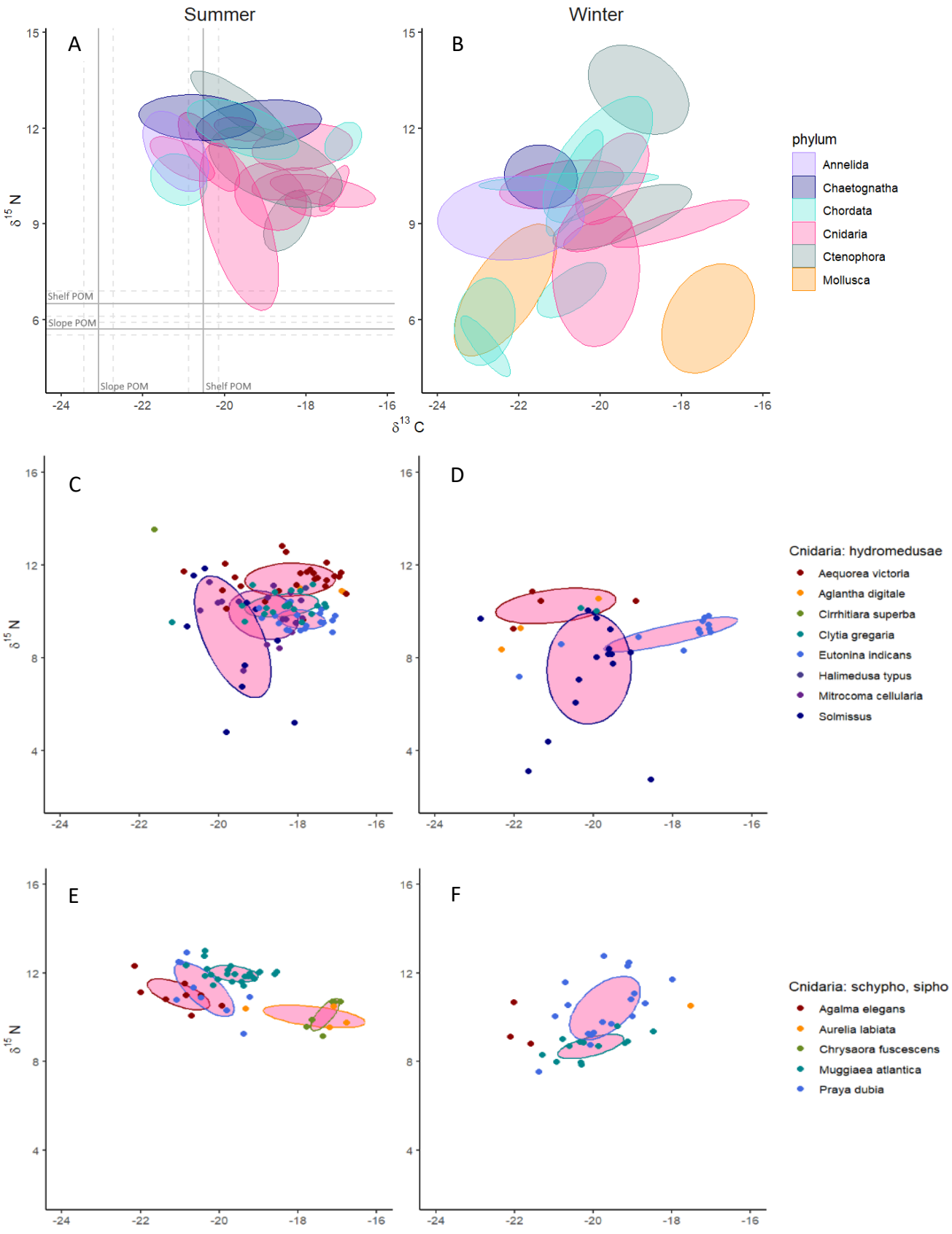
The isotopic values of samples collected in summer and winter were significantly different both in $\delta^{13}C$ and $\delta^{15}N$ separately (Welch's two-sample t-test, $\delta^{13}C$ $p<0.001$, $\delta^{15}N$ $p<0.001$), and with $\delta^{13}C$ and $\delta^{15}N$ considered together (Permanova, 999 perm, df=1, SumOfSquares=795.0, F=115.87, $R^2=0.17748$, $p<0.001$) (Figure 2).

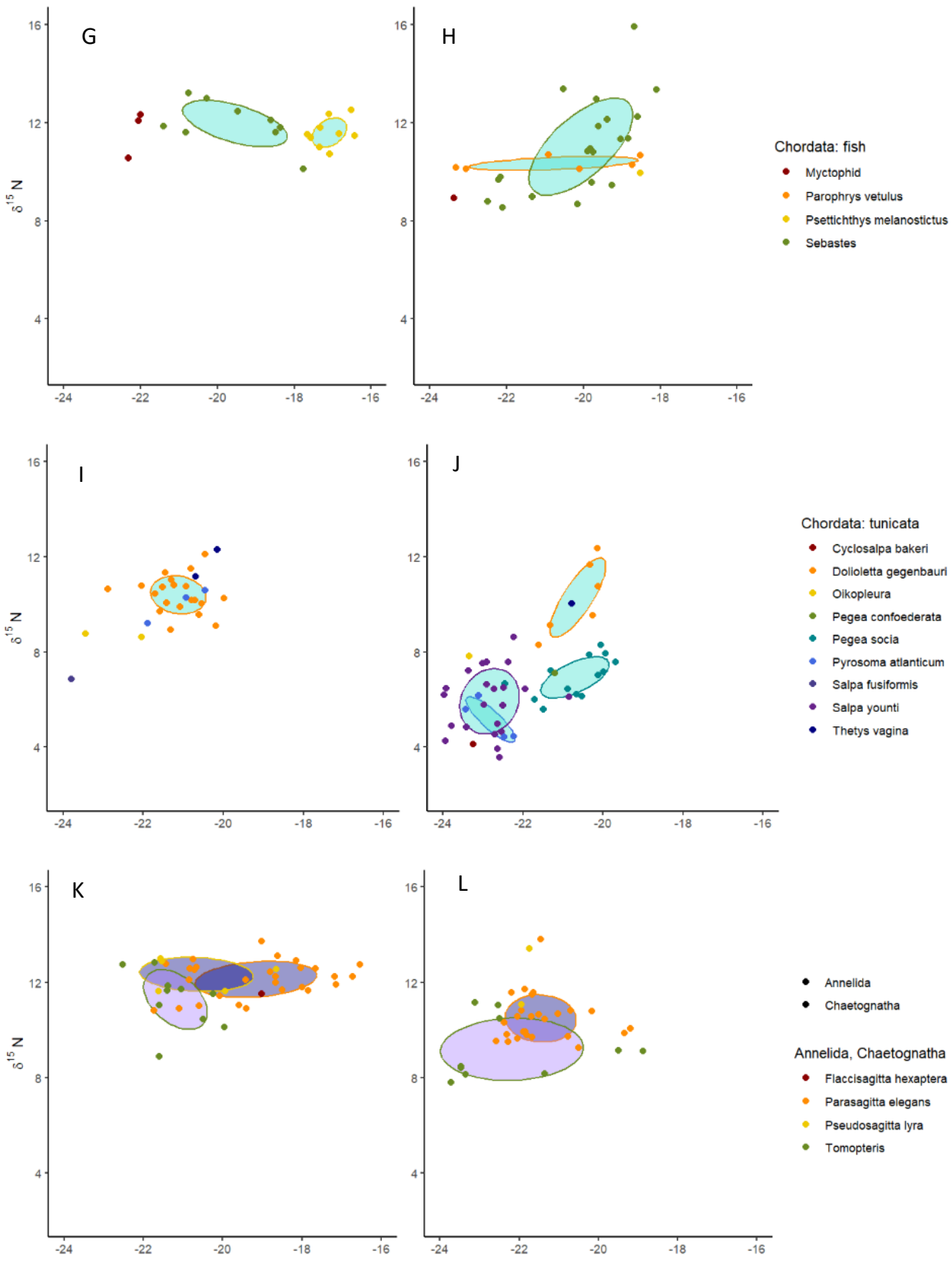
There were significant differences in isotope values between each season/region combination (summer-shelf, summer-offshore, winter-shelf, winter-offshore) (Permanova, 999 perm, df=3, SumOfSquares=1338.9, F=76.517, R^2=0.30222, p<0.001). Each was significantly different from each of the others (pairwise Permanova, p<0.005, fdr adjustment). Comparing $\delta^{13}C$ and $\delta^{15}N$ separately, all season/regions were significantly different for both isotopes (pairwise t-test, p<0.05, fdr adjustment) (Figure 2).

Species comparisons

In both seasons, there was a significant difference in isotope values between species. (Summer: Permanova, 999 perm, df=29, SumOfSquares=801.36, F=14.28, R^2=0.615, p<0.001) (Winter: Permanova, 999 perm, df=27, SumOfSquares=1633.81, F=17.953, R^2=0.689, p<0.001).

In summer, the species with the lowest $\delta^{15}N$ values was *Solmissus spp.,* and the species with the highest $\delta^{15}N$ values was *Beroe spp.* followed by *Parasagitta elegans, Pseudosagitta lyra*, and *Sebastes spp*. The species with the lowest $\delta^{13}C$ were *Pseudosagitta lyra, Agalma elegans, Tomopteris spp.*, and *Dolioletta gegenbauri*. The species with the highest $\delta^{13}C$ were *Aurelia labiata* and *Psettethichtys melanostictus* (Figure 3A). When each of the 29 species was compared to each other species (yielding 435 comparisons), 191 species pairings had significant differences (44% of the comparisons) (pairwise Permanova, p<0.05, fdr adjustment). The five pairings with the largest pseudo-f-statistics (a ratio of between-group variability to within-group variability indicating the most different from each other) were: *Eutonina indicans-Muggiaea atlantica* (F=173.24), *Dolioletta gegenbauri-Eutonina indicans* (F=133.04), *Dolioletta gegenbauri-Psettetichthys melanostictus* (F=121.57), *Psettichthys melanostictus-Salpa fusiformis* (F=116.62), and *Oikopleura spp.-Psettitchthys melanostictus* (F=115.36). The five species pairings with the lowest pseudo-f-statistics were: *Muggiaea atlantica-Sebastes spp.* (F=0.05), *Aequorea victoria-Halimedusa typus* (F= 0.12), *Flaccisagitta hexaptera-Parasagitta elegans* (F= 0.13), *Flaccisagitta hexaptera-Pleurobrachia bachei* (F=0.14), and *Flaccisagitta hexaptera-Sebastes spp.* (F=0.17).


Summer
Winter
A
B
C
D
E
F
Shelf POM
Slope POM
Slope POM
Shelf POM
δ15 N
δ13 C
phylum
Annelida
Chaetognatha
Chordata
Cnidaria
Ctenophora
Mollusca
Cnidaria: hydromedusae
Aequorea victoria
Aglantha digitale
Cirrhitiara superba
Clytia gregaria
Eutonina indicans
Halimedusa typus
Mitrocoma cellularia
Solmissus
Cnidaria: schypho, sipho
Agalma elegans
Aurelia labiata
Chrysaora fuscescens
Muggiaea atlantica
Praya dubia


G
H
I
J
K
L
δ15 N
16
12
8
4
-24
-22
-20
-18
-16
Chordata: fish
Myctophid
Parophrys vetulus
Psettichthys melanostictus
Sebastes
Chordata: tunicata
Cyclosalpa bakeri
Dolioletta gegenbauri
Oikopleura
Pegea confoederata
Pegea socia
Pyrosoma atlanticum
Salpa fusiformis
Salpa younti
Thetys vagina
Annelida
Chaetognatha
Annelida, Chaetognatha
Flaccisagitta hexaptera
Parasagitta elegans
Pseudosagitta lyra
Tomopteris

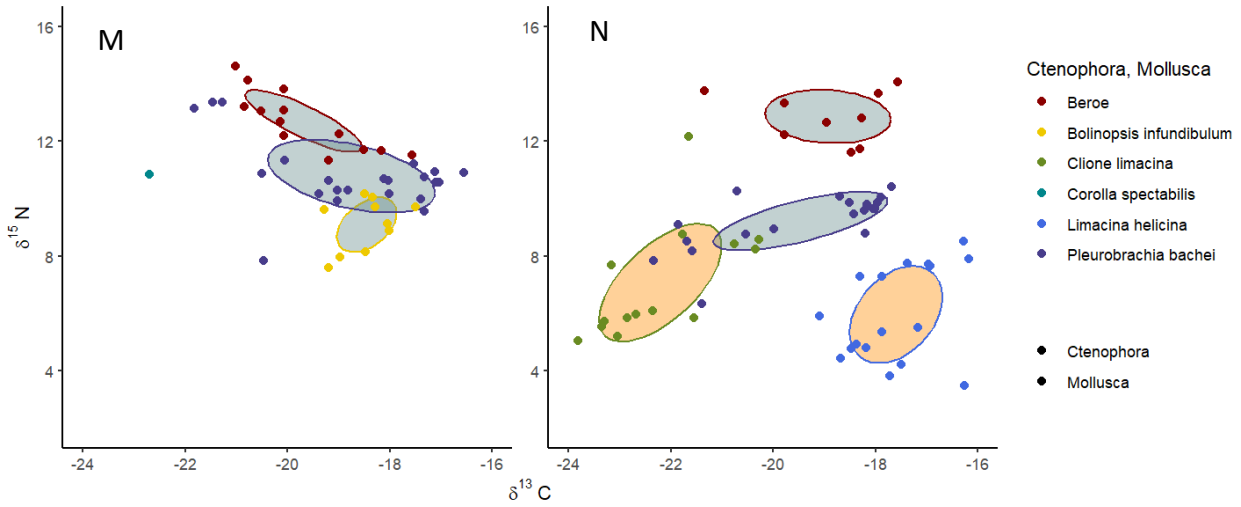


Figure 3: Crossplot of $\delta^{13}C$ and $\delta^{15}N$ values of all gelatinous zooplankton (and larval fish) samples separated by species. A) and B) show 40% ellipses of each species in summer and winter, respectively, colored by phylum. Gray lines are NCC summer particulate organic matter $\delta^{13}C$ from Miller et al., (2008) and $\delta^{15}N$ from Miller et al., (2010). C) though N) show each sample (dots) and species (40% ellipses) separted by season and phylum or lower taxonomic group. Dot and outline color indicate species, and ellispe fill color indicates phylum. C) and D) are hydromedusae (phylum Cnidaria), E) and F) are scyphomedusae and siphonophores (phylum Cnidaria), G) and H) are fish (phylum Chordata), I) and J) are tunicates (phylum Chordata), K) and L) are phyla Annelida and Chaeotgnatha, and M) and N) are phyla Ctenophora and Mollusca.

In winter, the lowest $\delta^{15}N$ values belonged to *Salpa younti*, *Pyrosoma atlanticum*, *Clione limacina*, and *Limacina helicina*, followed by *Solmissus spp*. *Beroe spp.* had the highest $\delta^{15}N$ values followed by *Sebastes spp*. The species with the lowest $\delta^{13}C$ values were *Salpa younti*, *Pyrosoma atlanticum, Clione limacina*, and *Tomopteris spp.*, while the taxa with the highest $\delta^{13}C$ values were *Limacina helicina* and *Eutonina indicans* (Figure 3B). When each of the 27 species was compared to every other species (yielding 378 comparisons), 129 species pairings had significant differences (34% of the pairings) (pairwise Permanova, $p<0.05$, fdr adjustment). The five pairings with the largest pseudo-f-statistics (most different) were: *Clytia gregaria-Cyclosalpa bakeri* (F=339.72), *Beroe spp.-Salpa younti* (F=177.96), *Limacina helicina-Parasagitta elegans* (F=149.04), *Parasagitta elegans-Salpa younti* (F= 134.79), and *Praya dubia-Salpa younti* (F= 117.95). The five pairings with the lowest pseudo-f-statistics were: *Aequorea victoria – Parophrys vetulus* (F= 0.03), *Dolioletta gegenbauri – Thetys vagina* (F= 0.03), *Aequorea victoria – Thetys vagina* (F= 0.02), *Dolioletta gegenbauri – Parophrys vetulus* (F= 0.02), and *Parophrys vetulus – Thetys vagina* (F=0.02).

Seasonal shifts

We compared summer vs. winter within species for all species that had at least three samples (the minimum sample size for ellipse estimation) in each season in one or both of the shelf/offshore regions. On the shelf, a majority of species (six out of eight) had higher $\delta^{13}C$ and $\delta^{15}N$ in the summer compared to winter. The largest seasonal shifts were 3.29‰ $\delta^{15}N$ in *Muggiaea atlantica* and 3.07‰ $\delta^{13}C$ in *Parasagitta elegans*. *Sebastes spp.* was the only species that had higher $\delta^{13}C$ but lower $\delta^{15}N$ in summer compared to winter. *Praya dubia* was the only species that had lower $\delta^{13}C$ and $\delta^{15}N$ in summer compared to winter (Figure 4A). The majority of species (six out of eight) also had standard ellipse areas smaller in summer compared to winter, (though this was a different six than the six that had similar isotope shifts.) The two species that had larger standard ellipse areas in summer compared to winter were *Clytia gregaria* (0.875 ± 0.39(sd) ‰^{2} difference) and *Parasagitta elegans* (0.415 ± 0.789(sd) ‰^{2} difference). The largest change in standard ellipse area between seasons was by *Solmissus spp.*, which had a standard ellipse area 15.16 ± 14.36 (sd) ‰^{2} larger in winter compared to summer (Figure 4C).

Offshore, most species (seven out of twelve) had higher $\delta^{13}C$ and $\delta^{15}N$ in summer compared to winter, and four had higher $\delta^{13}C$ but lower $\delta^{15}N$ in summer compared to winter. Only one species, *Beroe spp.* had lower $\delta^{15}N$ in summer compared to winter, and it also had lower $\delta^{13}C$ in summer. The largest shifts were 4.59‰ $\delta^{15}N$ by *Pyrosoma atlanticum* and 2.52‰ $\delta^{13}C$ by *Aequorea victoria*, both of which had larger isotope values in summer (Figure 4B). Seven species also had standard ellipse areas larger in winter than summer, (though this was a different seven species than those that had larger $\delta^{13}C$ in summer compared to winter.) The largest standard ellipse area shift was by *Pleurobrachia bachei*, which was 11.95 ± 6.54(sd) ‰^{2} larger in summer compared to winter (Figure 4D).

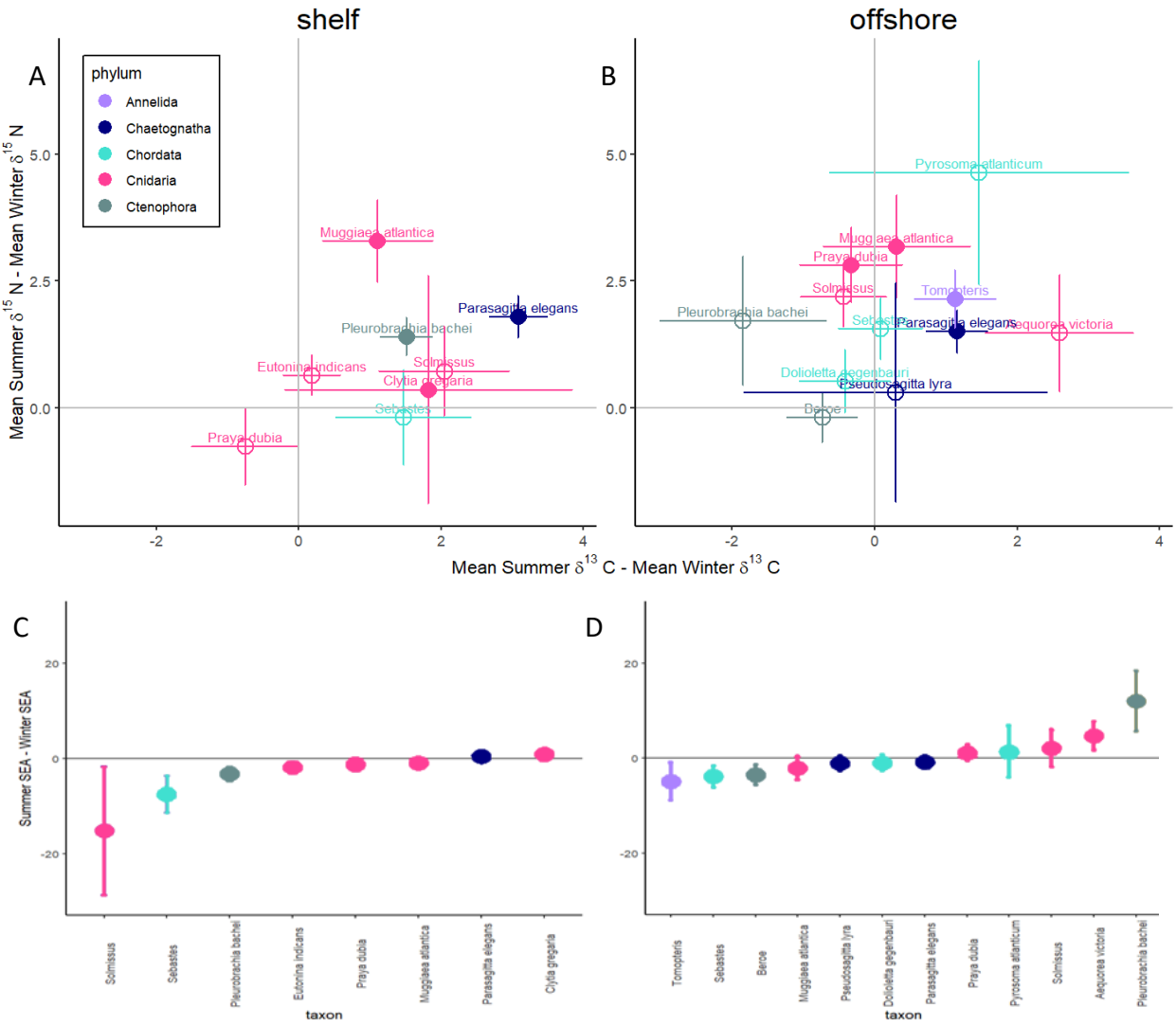


Figure 4. Seasonal shifts in resource use by gelatinous zooplankton species. A) and B) show the differences in Bayesian estimates of mean $\delta^{13}C$ and $\delta^{15}N$ values between summer and winter on the shelf and offshore, respectively. Solid dots are species with significantly different isotope values between the summer and winter (Permanova on original data, $p<0.05$). Error bars are one standard deviation of the difference in the Bayesian mean estimates. C) and D) show the differences in standard ellipse area between summer and winter on the shelf and offshore, respectively. Error bars are one standard deviation of the difference in Bayesian ellipse area estimates. Colors indicate phylum.

Comparison of feeding modes

We grouped the species into seven feeding modes adapted from Kiørboe, (2011) (Figure 5A, appendix table S1). The relative positions of all feeding modes were similar between summer and winter (Figure 5B,C). Winter standard ellipse areas were larger than summer for all feeding modes except current feeding with tentacles (and current feeding with lobes which only was present in the summer) (Figure 5B,C).

In summer, the isotope values of all seven feeding modes were significantly different from each other (pairwise Permanova, fdr adjustment, $p<0.05$) except active ambush with mouth / cruise feeding with mouth and current feeding with lobes / cruise feeding with tentacles (see appendix table S2 for all comparisons). Cruise feeding with mouth and active ambush with mouth had the highest $\delta^{15}N$ values, and cruise feeding with tentacles had the lowest $\delta^{15}N$ values. Suspension feeding had the lowest $\delta^{13}C$ values and cruise feeding with tentacles and cruise feeding with the mouth had the highest $\delta^{13}C$ values (Figure 5B). Cruise feeding with tentacles (only *Solmissus spp.*) had the largest standard ellipse area followed closely by suspension feeding, and current feeding with lobes (only *Bolinopsis spp.*) had the smallest standard ellipse area (Figure 5D).

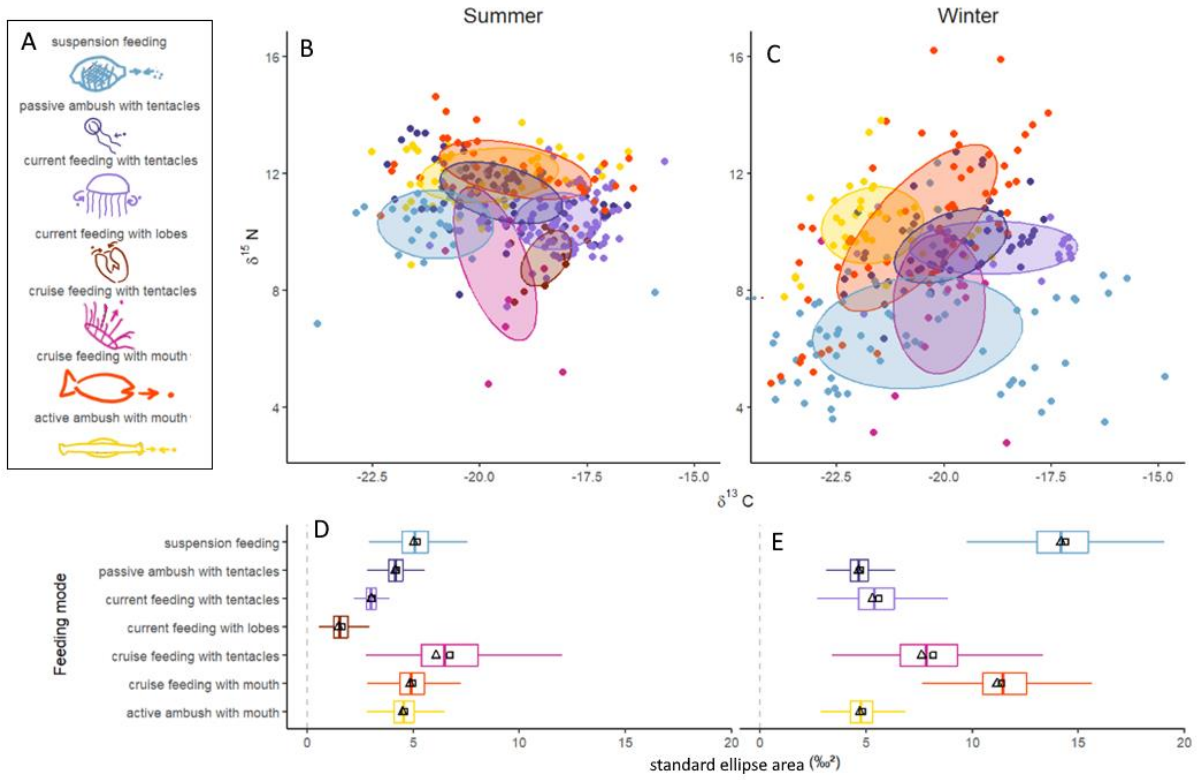


Figure 5. Resource use by feeding mode. A) Diagram of seven feeding modes used by gelatinous zooplankton, colored to correspond to the other panels in the figure. B) and C) show the $\delta^{13}C$ and $\delta^{15}N$ of each gelatinous zooplankton sample colored by feeding mode, with 40% standard ellipse areas drawn for each feeding mode in summer and winter, respectively. D) and E) show the standard ellipse areas for each feeding mode in summer and winter, respectively. The boxplots show the Bayesian standard ellipse area measurements, the triangles show the standard ellipse area calculated conventionally, and the squares show the conventional standard ellipse area corrected for sample size. All standard ellipse area calculations were conducted using the SIBER package in R.

In winter, there were six feeding modes represented because cruise feeding with lobes (*Bolinopsis spp.*) was not collected. All six feeding modes were significantly different from each other (pairwise Permanova, fdr adjustment, $p<0.05$) except active ambush with mouth / cruise feeding with mouth and cruise feeding with tentacles / suspension feeding. (See appendix table S3 for all comparisons.) Cruise feeding with mouth had the highest $\delta^{15}N$ and suspension feeding had the lowest $\delta^{15}N$. Suspension feeding and active ambush with mouth had the lowest $\delta^{13}C$ and current feeding with tentacles had the highest $\delta^{13}C$ (Figure 5C). Suspension feeding had the largest standard ellipse area followed by cruise feeding with tentacles, and current feeding with tentacles had the smallest standard ellipse area (Figure 5E).

Discussion

Gelatinous zooplankton living in the Northern California Current eastern boundary upwelling zone experience seasonally and spatially dynamic conditions. The 36 species examined here, 32 gelatinous zooplankton and 4 larval fish, represent the broadest range of gelatinous species ever analyzed for stable isotope composition. These species covered a wide trophic range exhibited by their $\delta^{13}C$ and $\delta^{15}N$ values, which varied between samples collected in summer vs. winter. Individual species occupied isotopically distinct niches, with more species having significantly different isotope values from each other in the summer compared to the winter. In summer, most species also had higher $\delta^{15}N$ values and smaller standard ellipse areas than in winter. When species were grouped by feeding mode, the seven feeding modes exhibited distinct isotope values with the exception of cruise feeding with a mouth and active ambush with a mouth. These findings highlight the trophic variety and dynamism of less-studied gelatinous species in this highly productive ecosystem and emphasize the unique roles of these species in marine food webs.

The overall gelatinous zooplankton isotope space is large

Gelatinous zooplankton are a highly diverse group whose members occupy many roles in marine food webs, reflected in the large $\delta^{13}C$ - $\delta^{15}N$ isotope space they occupy. The stable isotope ranges of the gelatinous zooplankton in this study, 9.19‰ for $\delta^{13}C$ and 13.44‰ for $\delta^{15}N$, equate to roughly 3.95 trophic levels assuming a commonly-used trophic discrimination factor of 3.4‰ for $\delta^{15}N$ (Post, 2002), or 6.4 trophic levels assuming a scyphozoan-specific trophic

discrimination factor of 2.1‰ for $\delta^{15}N$, or 7.73 trophic levels using a scyphozoan-specific trophic discrimination factor of 1.7‰ for $\delta^{15}N$ (Schaub et al., 2021). Our stable isotope ranges are ~1‰ larger than the $\delta^{13}C$ and $\delta^{15}N$ ranges in gelatinous zooplankton in the tropical east Atlantic, though the highest $\delta^{15}N$ values there were in samples below 400m depth (Chi et al., 2021). The $\delta^{15}N$ range we found among summer gelatinous zooplankton samples, 9.83‰, was 0.4‰ higher than the range reported for particulate organic matter to apex predator soupfin sharks (*Galeorhinus galeus*) previously recorded in this region in the summer (Miller et al., 2010).

An estimate of 4-7 trophic levels for gelatinous zooplankton is not unreasonable. This group is known to include microbe-eating suspension feeders (ex. pyrosomes, Schram et al., 2020; doliolids, Steinman et al., 2024), predators of herbivorous copepods or other herbivorous crustacean zooplankton (ex. *Muggiaea atlantica* siphonophores, Purcell, 1982), predators of secondary consumers whose diets include chaetognaths and fish (ex. siphonophores, Damian-Serrano et al., 2022), taxa whose diets include fish eggs which have elevated $\delta^{15}N$ (ex. siphonophores, ctenophores, medusae, Purcell & Arai, 2001), and "medusavores" which consume other gelatinous zooplankton and may even exhibit cannibalism, allowing the food chain to be extended greatly (ex. *Solmissus spp.* hydromedusae, Raskoff, 2002; *Aequorea victoria* hydromedusae, Purcell, 1991). The large range of trophic levels we observed in the stable isotope values of gelatinous zooplankton, as large a range as from primary producers to apex predators, is expected from prior studies of gelatinous zooplankton. However, this trophic diversity is still underappreciated in the broader marine ecology community (Pauly et al., 2008). Gelatinous zooplankton are rarely included in global food web models (Luo et al., 2020; Wright et al., 2021), and multiple gelatinous groups are almost never considered. Including these diverse organisms in trophic models could substantially revise our understanding of marine food web functioning.

Presence/absence of suspension feeders seasonally influences overall gelatinous trophic space

Despite wider ranges of isotope values in winter compared to summer, in general the relative positions of species were similar in both seasons, suggesting no major restructuring of the gelatinous food web between seasons (Figure 3A,B). This is consistent with the zooplankton food web in the Sea of Okhotsk (northwest Pacific) (Gorbatenko et al., 2014). However, the presence and absence of different species in each season changed the isotope space of the

gelatinous food web overall. Notably, three low- $\delta^{15}N$ species that feed on suspended particles (Conley et al., 2018) – *Salpa younti* and *Pegea socia* salps and *Limacina helicina* pteropods – were present in our study in substantial numbers but were collected almost exclusively in the winter (appendix Figure S2). The low $\delta^{15}N$ of these species suggests that their diets include bacteria and primary-producers, though isotope values of specific microbe and phytoplankton groups are not well understood (but see Rau et al., 1990; Fawcett et al., 2011). These gelatinous species could change the structure of the food web when they are present by directly consuming microbes and primary producers.

The range of $\delta^{15}N$ and $\delta^{13}C$ values within each cast, a proxy for the gelatinous food chain length, was larger in winter than in summer offshore as well as on the shelf (appendix Figure S3). This is consistent with the general understanding that lower productivity conditions lead to longer food chains (Ryther 1969). However, in our study, this expanded food chain length is likely due in part to the presence of low trophic level suspension feeders, which fill a trophic role that was otherwise occupied by non-gelatinous taxa. Therefore, in winter low-productivity conditions, where longer food chains may lead to less efficient energy transfer to higher trophic levels, the presence of gelatinous suspension feeders could alter the traditional food web pathways by making small particles directly available to larger predators, increasing the efficiency of energy and biomass transfer within ecosystems (Sutherland & Thompson, 2021; Stukel et al., 2024).

Resource competition is not a major driver of species distributions

When each species' isotope values were compared with each other species within each season, 44% of species pairings had significant differences in summer while 34% had significant differences in winter. This suggests a low degree of difference in resource use between species in both seasons, but particularly among species with mid-range isotope values (consumers of small zooplankton such as copepods) in winter (Figure 3B).

If species must compete for resources, they might be unlikely to occur at the same place and time. Conversely, species requiring the same resources might "flock" towards patches of these resources (Folt & Burns, 1999). To test whether the difference in food resources between two species, represented by their stable isotope values, was related to the degree to which the two species co-occurred, we investigated the correlation between the pseudo-f-value and a co-occurrence ratio calculated for each species pair. The pseudo-f-value is a measure of the

difference between two groups of isotope values (the ratio of between-species variation to within-species variation), and the co-occurrence ratio was the number of net casts where the two species were both collected divided by the number of times the less abundant species was collected, which was the highest possible number of times the two species could co-occur (Figure 6).

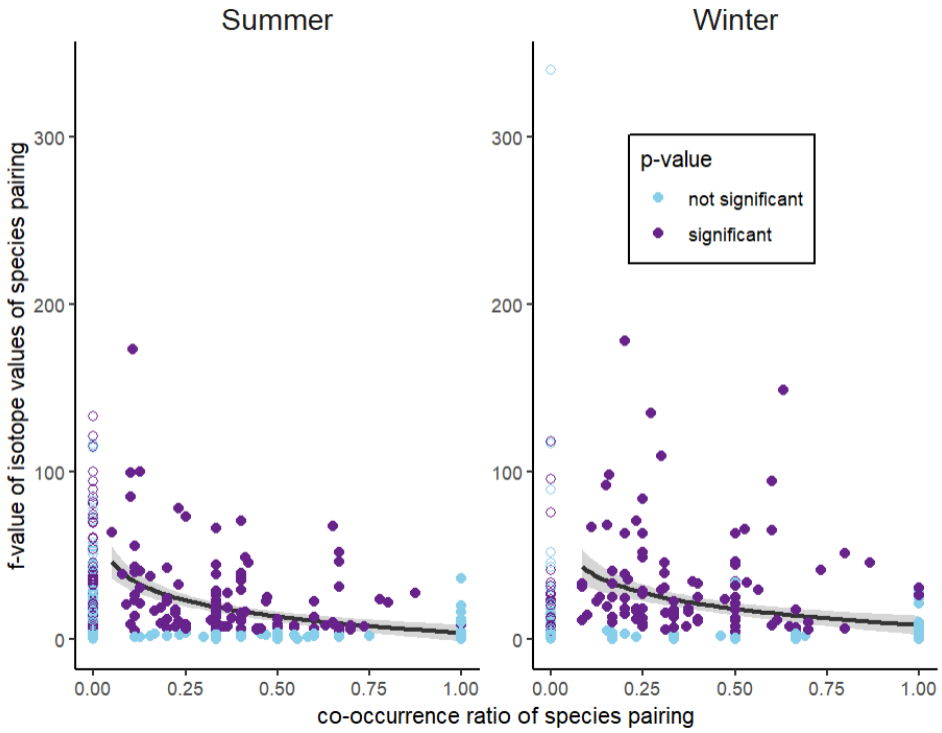


Figure 6. Scatter plots of the co-occurrence ratio of species pairs vs. the pseudo-f-values of species pairs. Each point represents one species pair, and points are colored by p-values>0.05 (blue) and p-values<0.05 (purple). A) shows species collected in summer and B) shows species collected in winter. Black lines are logarithmic models of the form y=a*ln(x)+b. Species pairs with a co-occurrence ratio of zero (were never collected together) are marked in hollow circles and are not included in the logarithmic model.

Logarithmic models of the co-occurrence ration of species pairs and the pseudo-f-values of species pairs had an equation of y=-14.096*ln(x)+3.934 (multiple R^2=0.1827, p=1.298e-09) in the summer and y=-14.070*ln(x)+8.496 (multiple R^2=0.1208, p=1.246e-06) in the winter. This suggests that in both seasons species that were found together more often (high co-occurrence) had more similar stable isotope values (low pseudo-f-values), but the relationship is not strong (Figure 6). However, species pairs with similar isotope values could occur at any degree of co-occurrence, while the species pairs with very different stable isotope values were more likely to be found in species that do not occur together, likely due to spatial variation in isotopic baselines

leading to more difference in isotope values among samples collected far apart. While species co-occurrence and stable isotope value similarity are only slightly related, the relationship suggests that species using similar resources could occur together as readily as they occurred separately, and therefore that competition for food resources was not a driving factor of species distributions (Hebert, 1982).

Seasonal shifts in isotope values vary by species

Many of the gelatinous zooplankton species had different $\delta^{13}C$ and $\delta^{15}N$ values between the summer and winter. Three primary causes of differences in stable isotope values are shifts in the baseline values of phytoplankton affecting the whole ecosystem, changes in food chain length affecting the whole ecosystem, and changes in diet affecting species individually. We expected seasonal differences in $\delta^{13}C$ and $\delta^{15}N$ baselines due to differences in phytoplankton growth and utilization of nitrate and dissolved inorganic carbon in summer and winter (McMahon et al., 2013). Higher $\delta^{13}C$ on the high-productivity shelf compared to the low-productivity offshore region has been observed in this area in the summer (Miller et al., 2008), consistent with the relationship we expected between increased phytoplankton growth and increased (less negative) $\delta^{13}C$. As for $\delta^{15}N$, in the summer on the shelf particulate organic matter has been observed to have slightly higher (by less than 1‰) $\delta^{15}N$ than on the continental shelf slope, but no difference was observed in copepods or decapod larvae (Miller et al, 2010), highlighting the complex relationship between productivity and $\delta^{15}N$. To our knowledge, no previous studies have analyzed stable isotope composition of any organisms in the Northern California Current during winter. In the Sea of Okhotsk in the northwest Pacific, which also experiences summer upwelling (Zhabin et al., 2019), $\delta^{13}C$ was higher on the shelf compared to offshore, and summer had higher $\delta^{13}C$ and lower $\delta^{15}N$ compared to spring or fall (Gorbatenko et al. 2014).

Our study area had contrasting conditions between the shelf and offshore regions, necessitating separation of these regions to fully understand the seasonal shifts in isotope values experienced by gelatinous zooplankton. On the shelf, chlorophyll fluorescence was higher in the summer than in the winter, indicative of higher phytoplankton growth in summer (Figure 1C), so we expected higher $\delta^{13}C$ in the summer compared to winter. The seawater surface nitrate on the shelf was higher in the summer than the winter (Forgrave et al., in review), so we expected $\delta^{15}N$ to be lower in the summer due to preferential uptake in lighter 14-N. In the offshore region,

phytoplankton growth was similarly low in both seasons (Figure 1C), so we expected similar $\delta^{13}C$ in both seasons. Seawater surface nitrate offshore was lower in summer than winter (Forgrave et al., in review), so we expected higher $\delta^{15}N$ in the summer compared to the winter.

In our study, one primary pattern was higher $\delta^{13}C$ and $\delta^{15}N$ in the summer compared to the winter for most species on the shelf (Figure 5A). Offshore, we observed higher $\delta^{15}N$ in the summer compared to the winter for most species, but some species had higher $\delta^{13}C$ in the winter and some had higher $\delta^{13}C$ in the summer (Figure 5B). These general seasonal shifts in isotope values were consistent with the direction of shifts predicted for the isotopic baseline, with the exception of the higher $\delta^{15}N$ we observed in the summer compared to the winter on the shelf. The overall $\delta^{15}N$ shift we observed also cannot be explained by an ecosystem-wide change in food chain length, because we would expect the high-productivity summer to have a shorter food chain length (Ryther 1969) and consequently lower $\delta^{15}N$ values compared to winter, opposite from what we observed. This seasonal shift in $\delta^{15}N$ values could indicate that surface nitrate during upwelling events comes from water with an enriched deep-water $\delta^{15}N$ signature (Saino & Hattori, 1980). Overall, the seasonal shifts in isotope values in gelatinous zooplankton in our study followed the shifts expected in the phytoplankton baseline, with the exception of the $\delta^{15}N$ on the shelf being mysteriously higher in the summer. However, the magnitude of the $\delta^{13}C$ and $\delta^{15}N$ change varied between gelatinous zooplankton species, suggesting species-specific diet shifts between seasons.

Species with anomalous isotopic shifts suggest changing trophic roles

Though our data does not show the exact diets of organisms, the shifts in isotopic values can suggest diet shifts, especially for the species with anomalous changes in $\delta^{13}C$ and/or $\delta^{15}N$ between seasons. In the offshore region, *Beroe spp.* was the only species that had both lower $\delta^{13}C$ and lower $\delta^{15}N$ in summer (Figure 5B). *Beroe spp*. is a ctenophore which primarily consumes other ctenophores, particularly lobates such as *Bolinopsis spp.* when they are available (Swanberg, 1974). The seasonal isotopic shift in *Beroe spp.* could have been driven by a switch from a diet of low $\delta^{13}C$ and $\delta^{15}N$ *Bolinopsis spp.* in the summer to the higher $\delta^{13}C$ and $\delta^{15}N$ cydippid ctenophore *Pleurobrachia bachei* in the winter when *Bolinopsis spp.* was not present.

Sebastes spp. fish larvae was the only species on the shelf to have lower $\delta^{15}N$ in the summer compared to winter (Figure 5A). In the southern California Current, larval *Sebastes paucipinis* ate a diverse diet of larval euphausiids, copepod nauplii, dinoflagellates, tintinnids,

cladocerans, and diatoms (Sumida & Moser, 1984). If the only phytoplankton accessible to *Sebastes spp.* larvae were large cells such as diatoms, the larvae could be primarily eating these primary producers in the high-productivity summers but switching to small zooplankton in the winters when large phytoplankton were less abundant. Despite the many factors influencing stable isotope values, we can hypothesize diet shifts from these data in species key to the ecosystem.

High productivity correlates with specialized diets and less resource sharing

In addition to changing average diet between summer and winter, many species also changed the variety of dietary resources used, as exhibited by the change in their standard ellipse area between the seasons (Figure 5C,D). In both the shelf and offshore regions, a majority of species used a wider variety of resources in the winter. Overall, during winter the gelatinous zooplankton had lower isotope values, larger standard ellipse areas, more overlap between taxa, and longer food chains. This suggests that in these colder less-productive months gelatinous taxa were feeding on a wider variety of resources, and therefore they had less difference in resource use, and the overall gelatinous food chain length was expanded in part due to the presence of suspension feeders. In the high-productivity summer months we saw higher isotope values overall, smaller standard ellipse areas, more difference between species, and shorter food chains, suggesting that under these conditions the gelatinous zooplankton species were feeding on more specialized and differentiated diets, and that the lower trophic levels were occupied by non-gelatinous taxa.

Contrasting theories exist about the link between productivity and diet breadth – high productivity could lead to reduced diet breadth as food abundance allows species to subsist only their preferred prey alone, or high productivity could lead to increased diet breadth as species make use of all abundant resources (Lesser et al., 2020). Gelatinous zooplankton exhibited the former – narrower diet breadth and more diet difference between species in higher productivity conditions, consistent with seagrass fish (Lesser et al., 2020). Our observations contrast with the finding by Lerner et al., (2022) that higher productivity leads to diet variety and lower trophic levels in species with trophic levels above zooplankton in the Northeast Pacific. In gelatinous zooplankton with diverse feeding modes, we saw food webs that were simultaneously longer with wider and less differentiated species diets in low productivity conditions compared to high productivity conditions.

Gelatinous zooplankton isotope values group by feeding mode

We grouped species into seven feeding modes based on their anatomy and behavior of finding and consuming food (appendix table S1). Active ambush feeders with a mouth sit still wait to strike prey that is detected nearby (ex. chaetognaths, Feigenbaum, 1991), while cruise feeders with a mouth move about in the water until they encounter prey (ex. *Beroe spp.* ctenophores, Swanberg, 1974). Passive ambush feeders with tentacles sit stationary in the water column until prey hits the tentacles (ex. *Pleurobrachia bachei* ctenophores, Greene et al., 1986), while current feeders with tentacles entrain prey with the current they generate while swimming (ex. *Clytia gregaria* hydromedusae, Corrales-Ugalde & Sutherland, 2021). Cruise feeders with tentacles (ex. *Solmissus spp.* hydromedusae, Raskoff, 2002) decouple the swimming current from prey encounter. Current feeders with lobes (ex. *Bolinopsis spp.* ctenophores, Kiørboe 2011), draw prey into the space between feeding lobes using a weak feeding current. Finally, suspension feeders use a mucus mesh to collect particles from the water (Conley et al., 2018). The distinct isotope values of the seven feeding modes in both seasons show that these feeding modes do correspond with distinct trophic roles, with the exception of active ambush with a mouth and cruise feeding with a mouth. These two feeding modes, the only two employing a mouth to catch prey, did not have significantly different stable isotope values in either season, suggesting that they captured the same food resources. However, the larger standard ellipse area of cruise feeding with a mouth compared to active ambush with a mouth in winter suggests that under low-productivity conditions cruise feeding with mouth might allow for a wider variety of prey compared to active ambush with mouth.

Even though most of the other feeding modes had significantly different isotope values from each other, passive ambush with tentacles and current feeders with tentacles had similar isotope values (albeit with a statistically significant difference), suggesting similar prey. Differentiation between the trophic niches of these two feeding modes has been observed for hydromedusae (Costello & Colin, 2002), but our results suggest that grouping species into three feeding anatomy groups (mouths vs. tentacles vs. mucus mesh) for a majority of species could be a middle ground between grouping all gelatinous species together and dividing them into higher-resolution feeding mode or taxonomic groups.

Among the seven feeding modes, the largest standard ellipse area, representing diet variety, was found in cruise feeders with tentacles in the summer and suspension feeders in the

winter. In our sample set, cruise feeding with tentacles was represented only by *Solmissus spp.*, a hydromedusa which feeds by swimming with its tentacles ahead of its bell (Mills & Goy, 1988; Raskoff, 2002). In the Central California Current, *Solmissus spp.* and other narcomedusae were observed to have the greatest diversity of prey out of 84 gelatinous and non-gelatinous predators examined, and most of its prey were ctenophores and other gelatinous organisms (Choy et al., 2017). In comparison to these previous observations, the $\delta^{15}N$ of this feeding mode in our data is unexpectedly low, on par with suspension feeders (Figure 5A,B), suggesting that this mode of feeding may allow for capture and ingestion of small particles unaccounted for by past studies.

In the summer, the group of suspension feeders was primarily comprised of *Dolioletta gegenbauri* doliolids, which is why this group had higher $\delta^{15}N$ and a smaller ellipse area compared to winter, when salps and *Limacina helicina* pteropods were also abundant. Pyrosomes and multiple species of salp had low $\delta^{15}N$ and $\delta^{13}C$, while *Limacina helicina* had low $\delta^{15}N$ and high $\delta^{13}C$, and *Dolioletta gegenbauri* had low $\delta^{13}C$ and high $\delta^{15}N$ (Figure 3B), greatly expanding the standard ellipse area of this feeding mode group overall. The reason for *Limacina helicina*'s elevated $\delta^{13}C$ values is unknown – it could be due to having different diet selectivity from salps (Gilmer & Harbison, 1991; Hiebert et al., 2025) or maybe *Limacina helicina* $\delta^{13}C$ is not directly comparable to the other taxa even after correction for lipid content and for carbonate shells (see appendix Figure S1). Gorbatenko et al. (2014) found *Limacina helicina* to have lower $\delta^{13}C$ and $\delta^{15}N$ than other gelatinous zooplankton except appendicularians, which aligns with expectations and contrasts with our data. The high $\delta^{15}N$ of *Dolioletta gegenbauri* compared to other suspension feeders could come from a detritus-based diet (Frischer et al., 2021) and shows that doliolids can have a distinct diet from other suspension feeders. Overall, the diets of mucus mesh suspension feeders can be quite varied.

Additional sources of variability in stable isotope composition

This study examined variability across two seasons (summer vs. winter) and considered two broad regions (shelf vs. offshore). It did not consider interannual variability or fine-scale spatial variability, which could affect the stable isotope composition of gelatinous zooplankton. Interannual variability appeared even between the two years examined in this study – notably, the temperature differed greatly between the two summers (Figure 1B) and the gelatinous $\delta^{13}C$ values differed between the two winters (appendix Figure S4). The Northern California Current region also experiences significant variability on shorter timescales, namely the pulses in

upwelling and productivity driven by days-to-weeks-long winds (Hickey & Banas, 2003). The effects of this short-term variability on stable isotope values likely differ between gelatinous taxa whose lifespans vary and whose stable isotope turnover times are unknown (Pitt et al., 2009). On longer timescales, sources of interannual variability in the Northern California Current include El Niño, which causes elevated water temperature (Huyer & Smith, 1985) and decreased zooplankton biomass (Chelton et al., 1982) in the area, as well as the Pacific Decadal Oscillation which affects wind stress and water temperatures, and "abnormal" events such as marine heat waves (ex. Bond et al., 2015), in addition to long-term anthropogenic influences. These interannual features likely expanded the range of isotope values we recorded for each species found in multiple years, and the effect of these variations on the ecology of the organisms as well as the stable isotope values is complex and unknown.

One significant feature of fine-scale spatial variability unaccounted for in our study is the outflow from the Columbia River, which brings low-salinity high-nutrient water to the nearshore shelf area (Landry et al., 1989). In the summer, the river plume is pushed southward into Oregon waters and outward away from the coast, while in the winter the plume is pushed northward in tight to the coast. The land-sea interactions in this dynamic coastal area and their impact on gelatinous zooplankton food webs remain to be further explored.

Caveats of stable isotope analysis in understudied organisms

Ecological interpretations from stable isotope measurements rely on predictable patterns in bulk $\delta^{15}N$ and $\delta^{13}C$ in animal tissues. These patterns, such as the alteration of isotope composition between diet and consumer, have been well-tested in many taxa, but not in gelatinous zooplankton. In various systems studied, the change in stable isotope ratio from diet to consumer varies greatly (Post, 2002) and can even vary among closely related species of gelatinous zooplankton or in the same species of gelatinous zooplankton fed different diets (Schaub et al., 2021; D'Ambra et al., 2014). Another factor that could affect our measurements is the possibility of food items remaining in the guts of the organisms analyzed, as we did not intentionally fast the organisms prior to preservation (Hill & McQuade, 2011). Due to the low organic content in the gelatinous zooplankton, even a small amount of prey in the gut could have a significant impact on the isotope values. One abundant species, *Parasagitta elegans*, had empty guts when collected using the same method we employed (Alberding, 2023), and hydromedusae and ctenophore *Pleurobrachia bachei* collected using this same method had prey in their guts

only 43% and 54% of the time, respectively (Corrales-Ugalde et al., 2021, Masterman et al., in review). Additionally, the consistently low carbon contents (appendix Figure S6) led us to believe that gut contents were not a major contributor to the gelatinous zooplankton organic matter and isotope composition. Even though further controlled studies are needed to refine the use of stable isotope analysis in gelatinous zooplankton, our study shows the extremely wide range of stable isotope compositions among the diverse gelatinous zooplankton of the Northern California Current ecosystem.

Conclusion

The Northern California Current is a spatially and seasonally dynamic region that is home to abundant gelatinous zooplankton with diverse taxonomy, diets, and feeding modes. These gelatinous zooplankton span a wide range of $\delta^{13}C$ and $\delta^{15}N$ indicative of the many roles they play in the food web, and their trophic diversity is often underappreciated in conceptualizations of marine food webs and modelling studies. While the overall structure of the gelatinous food web is similar in the high productivity summer season and the low productivity winter season, other distinctions between summer and winter highlight the need to study gelatinous zooplankton trophic ecology across seasons: in winter the gelatinous food chain was lengthened by the presence of suspension feeders, and species had more variety in their diets, whereas in summer gelatinous taxa had more specialized diets within a shorter food chain. Additionally, gelatinous zooplankton feeding modes had distinct isotope values, showing that this trait-based approach may be an effective way to describe gelatinous trophic diversity. Overall, this study emphasizes the variety of trophic roles of gelatinous zooplankton and shows the complexity of these organisms' trophic dynamics across space and time. Incorporating gelatinous zooplankton into future food web studies will be necessary for understanding the roles and impacts of these organisms in highly productive eastern boundary current ecosystems and beyond.

APPENDIX

Supplementary methods

Some species had slight variations in the methods of sample preparation:

1. Some *Aurelia labiata* and one *Chrysaora fuscescens* were homogenized prior to wet weight measurements by pouring the thawed organism through a sieve then mixing with a whisk. Then, approximately 60mL of homogenized tissue was dried and processed.

2. Many *Praya dubia* simples were parts of colonies rather the entire colony, and different parts were not differentiated in our analyses.

3. *Limacina helicina* $\delta^{13}C$ was corrected for the carbonate shells of these thecosome pteropods. For each of five randomly selected grouped *L. helicina* samples, the shells of ten individuals were removed under a dissecting microscope. The remaining shell-free tissue was dried, processed, and analyzed alongside the samples with shells remaining. $\delta^{13}C$ of shell-free samples was lower than that of corresponding samples with shells by 2.292‰ (0.386‰ standard deviation) (appendix Figure S1). This difference is larger than the 0.9‰ decrease found by Pomerlau et al., (2014) using acidification for carbonate removal.

Supplementary Tables

Table S1. Feeding mode and phylum of each species.

Species	Phylum	Feeding mode
Parasagitta elegans	Chaetognatha	active ambush with mouth
Pseudosagitta lyra	Chaetognatha	active ambush with mouth
Flaccisagitta hexaptera	Chaetognatha	active ambush with mouth
Beroe spp.	Ctenophora	cruise feeding with mouth
Clione limacina	Mollusca	cruise feeding with mouth
Tomopteris spp.	Annelida	cruise feeding with mouth
Parophrys vetulus	Chordata	cruise feeding with mouth
Myctophid spp.	Chordata	cruise feeding with mouth
Sebastes spp.	Chordata	cruise feeding with mouth
Psettichthys melanostictus	Chordata	cruise feeding with mouth
Solmissus spp.	Cnidaria	cruise feeding with tentacles
Bolinopsis infundibulum	Ctenophora	current feeding with lobes
Aequorea victoria	Cnidaria	current feeding with tentacles
Aurelia labiata	Cnidaria	current feeding with tentacles
Chrysaora fuscescens	Cnidaria	current feeding with tentacles
Mitrocoma cellularia	Cnidaria	current feeding with tentacles

Eutonina indicans	Cnidaria	current feeding with tentacles
Clytia gregaria	Cnidaria	current feeding with tentacles
Muggiaea atlantica	Cnidaria	passive ambush with tentacles
Agalma elegans	Cnidaria	passive ambush with tentacles
Aglantha digitale	Cnidaria	passive ambush with tentacles
Halimedusa typus	Cnidaria	passive ambush with tentacles
Praya dubia	Cnidaria	passive ambush with tentacles
Cirrhitiara superba	Cnidaria	passive ambush with tentacles
Pleurobrachia bachei	Ctenophora	passive ambush with tentacles
Dolioletta gegenbauri	Chordata	suspension feeding
Salpa younti	Chordata	suspension feeding
Oikopleura spp.	Chordata	suspension feeding
Cyclosalpa bakeri	Chordata	suspension feeding
Salpa fusiformis	Chordata	suspension feeding
Pyrosoma atlanticum	Chordata	suspension feeding
Pegea socia	Chordata	suspension feeding
Thetys vagina	Chordata	suspension feeding
Pegea confoederata	Chordata	suspension feeding
Corolla spectabilis	Mollusca	suspension feeding
Limacina helicina	Mollusca	suspension feeding

Table S2. P-values of pairwise permanovas between each pair of feeding modes in the summer.

SUMMER	active ambush with mouth	cruise feeding with mouth	cruise feeding with tentacles	current feeding with lobes	current feeding with tentacles	passive ambush with tentacles
cruise feeding with mouth	0.1197					
cruise feeding with tentacles	0.001313	0.001313				
current feeding with lobes	0.001313	0.001313	0.188			
current feeding with tentacles	0.001313	0.001313	0.001313	0.001313		
passive ambush with tentacles	0.043105	0.0245	0.001313	0.001313	0.001313	
suspension feeding	0.001313	0.001313	0.003706	0.001313	0.001313	0.001313

Table S3. P-values of pairwise permanovas between each pair of feeding modes in the winter.

WINTER	active ambush with mouth	cruise feeding with mouth	cruise feeding with tentacles	current feeding with tentacles	passive ambush with tentacles
cruise feeding with mouth	0.078214				
cruise feeding with tentacles	0.001875	0.0045			
current feeding with tentacles	0.001875	0.012273	0.003333		
passive ambush with tentacles	0.001875	0.053077	0.001875	0.0175	
suspension feeding	0.001875	0.001875	0.139	0.001875	0.001875

Supplementary Figures

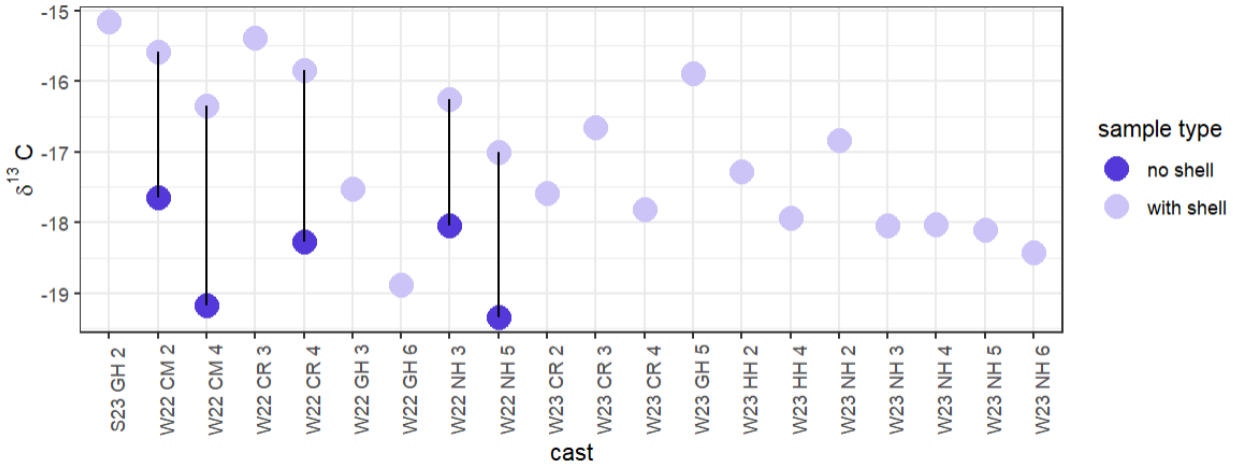


Figure S1. $\delta^{13}C$ values for each *Limacina helicina* sample. Color indicates whether organisms in the sample had shells (light purple) or had shells removed (dark purple). Vertical lines indicate pairs of shell and no-shell samples from the same groups of organisms.

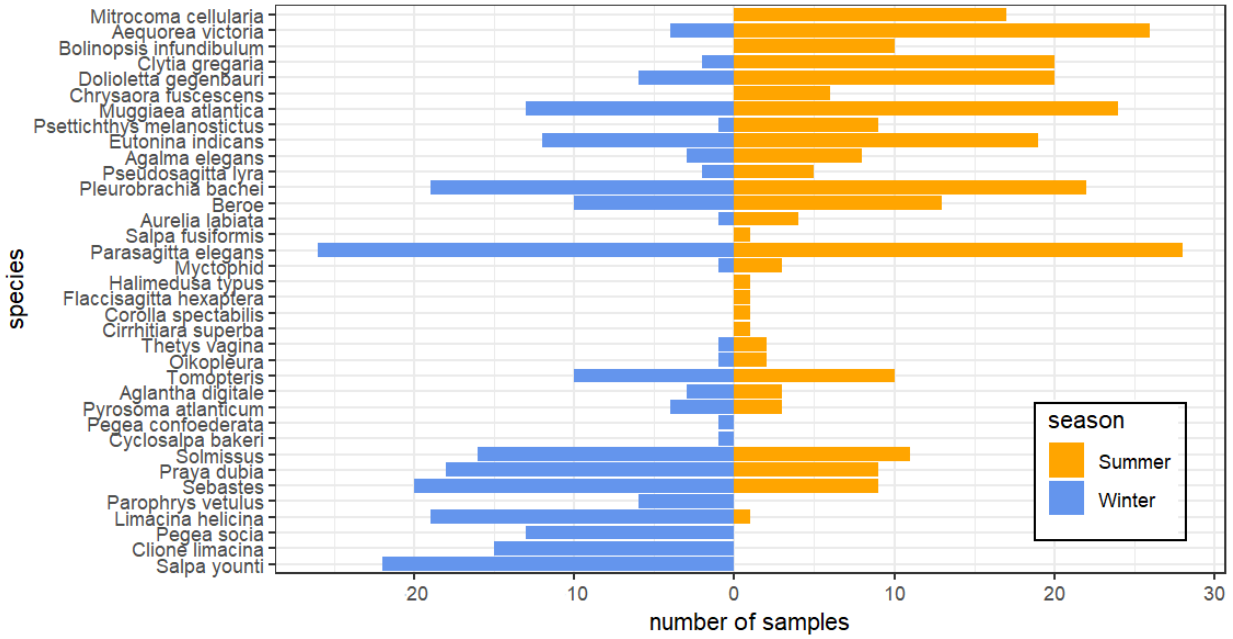


Figure S2. Bar plot of the number of samples (each sample is a group of one or more individuals) of each species collected in summer (orange) and winter (blue).

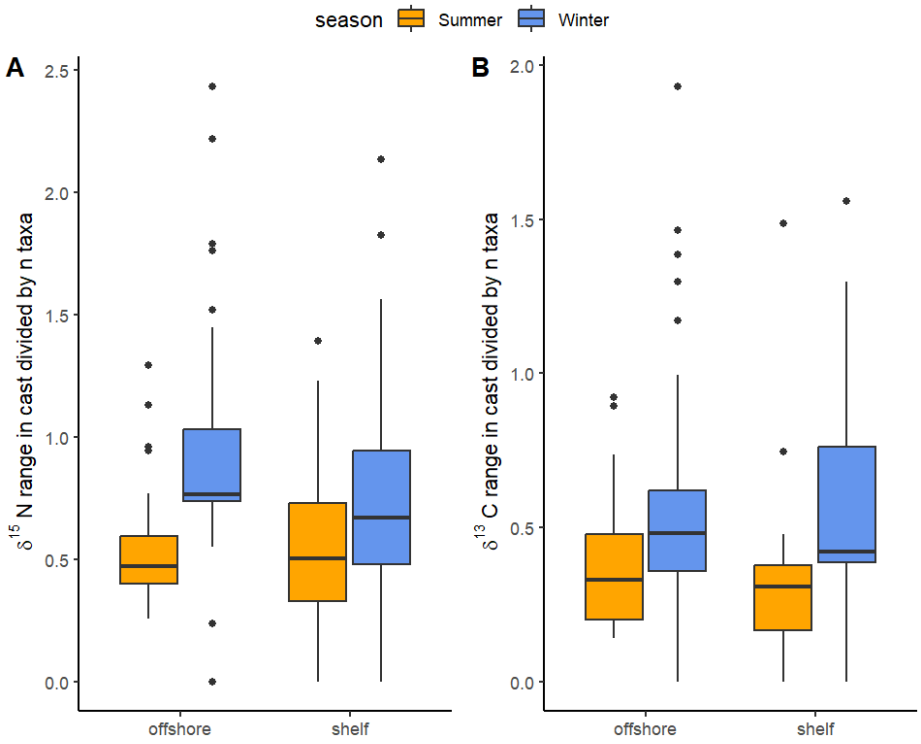


Figure S3. Boxplot of the range of A) $\delta^{15}N$ and B) $\delta^{13}C$ of samples collected in each net tow, divided by the number of species collected in the tow. Samples are separated by offshore vs. shelf region and colored by season.

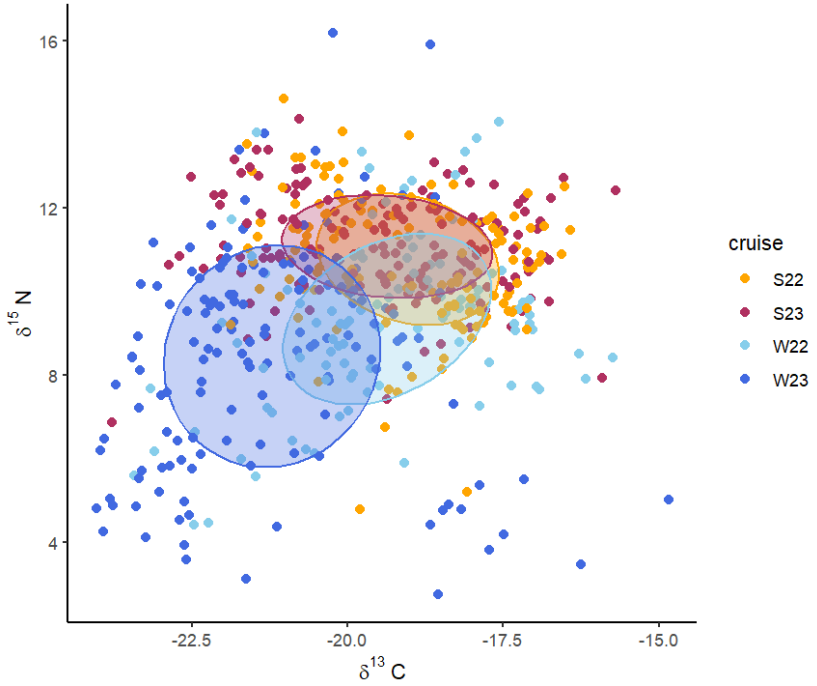


Figure S4. Crossplot of $\delta^{13}C$ and $\delta^{15}N$ of all gelatinous zooplankton and larval fish samples colored by sampling cruise. Shaded ellipses are 40% ellipses for each of the four sampling cruises.

Isotope values were different among the four cruises (Permanova, 999 perm, df=3, SumOfSquares=1070.7, F=56.339, R^2=0.2411, p<0.001). All four cruises were significantly different from each other (for summer 2022 vs. S23 p=0.039, for all other comparisons p=0.0012, fdr adjustment). Comparing $\delta^{13}C$ and $\delta^{15}N$ separately, $\delta^{13}C$ was not significantly different in summer 2022, summer 2023, and winter 2022 (pairwise t-tests, 999 permutations, p>0.05, fdr adjustment), but winter 2023 differed from the three other cruises (p<0.005). $\delta^{15}N$ was not significantly different between summer 2022 and summer 2023 (p>0.05), but winter 2022 and winter 2023 each differed from all other cruises (p<0.005).

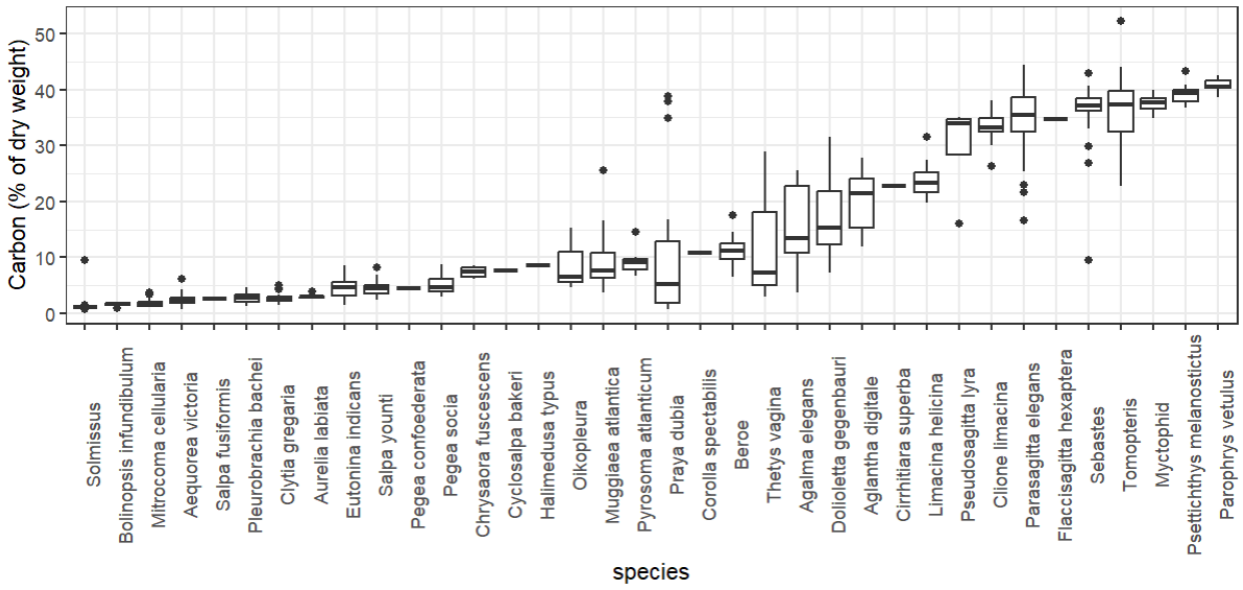


Figure S5. Boxplot of carbon contents of gelatinous zooplankton and larval fish samples. Carbon contents are the percentage of dry weight. In contrast, copepods contain ~40-60% carbon of dry weight (González et al., 2025)

REFERENCES CITED

Alberding, M. P. (2023). Chaetognaths in the California Current: High Resolution Relationships with Their Prey [Honors thesis, Wesleyan University]. Wesleyan University Digital Collections. doi:10.14418/wes01.1.2729

Bond, N.A., Cronin, M.F., Freeland, H. & Mantua, N. (2015) Causes and impacts of the 2014 warm anomaly. *Geophys. Res. Lett.*, **42**, 3414–3420. doi:10.1002/2015GL063306

Cavallo, C., Chiaradia, A., Deagle, B.E., McInnes, J.C., Sánchez, S., Hays, G.C. & Reina, R.D. (2018) Molecular analysis of predator scats reveals role of salps in temperate inshore food webs. *Front. Mar. Sci.*, **5**, 1–14. doi:10.3389/fmars.2018.00381

Chelton, D.B., Bernal, P.A. & McGowan, J.A. (2021) Large-scale interannual physical and biological interaction in the California Current. *J. Mar. Res.*, **40**, 1095–1125.

Chi, X., Dierking, J., Hoving, H., Lüskow, F., Denda, A., Christiansen, B., Sommer, U., *et al.* (2021) Tackling the jelly web: Trophic ecology of gelatinous zooplankton in oceanic food webs of the eastern tropical Atlantic assessed by stable isotope analysis. *Limnol. Oceanogr.*, **66**, 289–305. doi:10.1002/lno.11605

Choy, C.A., Haddock, S.H.D. & Robison, B.H. (2017) Deep pelagic food web structure as revealed by in situ feeding observations. *Proceedings. Biol. Sci.*, **284**. doi:10.1098/rspb.2017.2116

Conley, K.R., Lombard, F. & Sutherland, K.R. (2018) Mammoth grazers on the ocean's minuteness: a review of selective feeding using mucous meshes. *Proc. R. Soc. B Biol. Sci.*, **285**. doi:http://dx.doi.org/10.1098/rspb.2018.0056

Corrales-Ugalde, M. & Sutherland, K.R. (2021) Fluid mechanics of feeding determine the trophic niche of the hydromedusa Clytia gregaria. *Limnol. Oceanogr.*, **66**, 939–953. doi:10.1002/lno.11653

Corrales-Ugalde, M., Sponaugle, S., Cowen, R.K. & Sutherland, K.R. (2021) Seasonal hydromedusan feeding patterns in an Eastern Boundary Current show consistent predation on primary consumers. *J. Plankton Res.*, **43**, 712–724. doi:10.1093/plankt/fbab059

Costello, J.H. & Colin, S.P. (2002) Prey resource use by coexistent hydromedusae from Friday Harbor, Washington. *Limnol. Oceanogr.*, **47**, 934–942.

D'Ambra, I., Carmichael, R.H. & Graham, W.M. (2014) Determination of δ13C and δ15N and trophic fractionation in jellyfish: implications for food web ecology. *Mar. Biol.*, **161**, 473–480. doi:10.1007/s00227-013-2345-y

Damian-Serrano, A., Haddock, S.H.D. & Dunn, C.W. (2021) The evolution of siphonophore tentilla for specialized prey capture in the open ocean. *Proc. Natl. Acad. Sci.*, **118**. doi:10.1073/pnas.2005063118

Damian-Serrano, A., Hetherington, E.D., Anela Choy, C., Haddock, S.H.D., Lapides, A. & Dunn, C.W. (2022) Characterizing the secret diets of siphonophores (Cnidaria: Hydrozoa) using DNA metabarcoding. *PLoS One*, **17**, 1–24. doi:10.1371/journal.pone.0267761

Deniro, M. & Epstein, S. (1978) Influence of diet on the distribution of carbon isotopes in animals. *Geochim. Cosmochim. Acta*, **42**, 495–506. doi:10.1002/mop.25285

Dischereit, A., Beermann, J., Lebreton, B., Wangensteen, O.S., Neuhaus, S. & Havermans, C. (2024) DNA metabarcoding reveals a diverse, omnivorous diet of Arctic amphipods during the polar night, with jellyfish and fish as major prey. *Front. Mar. Sci.*, **11:1327650**. doi:10.3389/fmars.2024.1327650

Elton, C.S. (1927) *Animal Ecology.* Sidgwick and Jackson, London. Reprinted e.g. 2001, The University of Chicago Press. ISBN: 0-266-20639-4.

Fawcett, S.E., Lomas, M.W., Casey, J.R., Ward, B.B. & Sigman, D.M. (2011) Assimilation of upwelled nitrate by small eukaryotes in the Sargasso Sea. *Nat. Geosci.*, **4**, 717–722. doi:10.1038/ngeo1265

Feigenbaum, D. (1991). Food and Feeding Behavior. In Q. Bone, H. Kapp, & A. C. Pierrot-Bults (Eds.), *The Biology of Chaetognaths* (1st ed., pp. 45-54). Oxford Science Publications. ISBN: 9780198577157

Folt, C. & Burns, C. (1999) Biological drivers of zooplankton patchiness. *Trends Ecol. Evol.*, **14**, 300–305. doi:10.1016/S0169-5347(99)01616-X

Forgrave, K. E., Sweeny, C., Steinman, M., Kerkar, A., Pettit, T., & Thompson, A. W. (2025) Impact of oceanographic gradients and marine heatwaves on the phytoplankton community in the Northern California Current System. Manuscript submitted for publication.

Frischer, M.E., Lamboley, L.M., Walters, T.L., Brandes, J.A., Arneson, E., Lacy, L.E., López-Figueroa, N.B., *et al.* (2021) Selective feeding and linkages to the microbial food web by the doliolid Dolioletta gegenbauri. *Limnol. Oceanogr.*, **66**, 1993–2010. doi:10.1002/lno.11740

GEBCO Compilation Group (2024) GEBCO 2024 Grid (doi:10.5285/1c44ce99-0a0d-5f4f-e063-7086abc0ea0f)

Gilmer, R.W. & Harbison, G.R. (1991) Diet of Limacina helicina (Gastropoda: Thecosomata) in Arctic waters in midsummer. *Mar. Ecol. Prog. Ser.*, **77**, 125–134.

González, A.L., Merder, J., Andraczek, K., Brose, U., Filipiak, M., Harpole, W.S., Hillebrand, H., *et al.* (2025) StoichLife: A Global Dataset of Plant and Animal Elemental Content. *Sci. Data*, **12**, 569. doi:10.1038/s41597-025-04852-w

Gorbatenko, K.M., Lazhentsev, A.E. & Kiyashko, S.I. (2014) Seasonal Dynamics of the Trophic Status of Zooplankton in the Sea of Okhotsk (Based on Data from Stable Carbon and Nitrogen Isotope Analysis). *Russ. J. Mar. Biol.*, **40**, 519–531. doi:10.1134/S1063074014070025

Greene, C.H., Landry, M.R. & Monger, B.C. (1986) Foraging Behavior and Prey Selection by the Ambush Entangling Predator Pleurobrachia Bachei. *Ecology*, **67**, 1493–1501.

Haddock, S.H.D. (2007) Comparative feeding behavior of planktonic ctenophores. *Integr. Comp. Biol.*, **47**, 847–853. doi:10.1093/icb/icm088

Hays, G.C., Doyle, T.K. & Houghton, J.D.R. (2018) A Paradigm Shift in the Trophic Importance of Jellyfish? *Trends Ecol. Evol.*, **33**. doi:10.1016/j.tree.2018.09.001

Hebert, P.D.N. (1982) Competition in zooplankton communities. *Ann. Zoo. Fenn.*, **19**, 349–356.

Herve, M (2023). _RVAideMemoire: Testing and Plotting Procedures for Biostatistics_. R package version 0.9-83-7, <https://CRAN.R-project.org/package=RVAideMemoire>.

Hetherington, E.D., Kurle, C.M., Benson, S.R., Jones, T.T. & Seminoff, J.A. (2019) Re-examining trophic dead ends: Stable isotope values link gelatinous zooplankton to leatherback turtles in the California Current. *Mar. Ecol. Prog. Ser.*, **632**, 205–219. doi:10.3354/meps13117

Hetherington, E.D., Close, H.G., Haddock, S.H.D., Damian-serrano, A., Dunn, C.W., Wallsgrove, N.J., Doherty, S.C., *et al.* (2024) Vertical trophic structure and niche partitioning of gelatinous predators in a pelagic food web: Insights from stable isotopes of siphonophores. *Limnol. Oceanogr.*, 1–18. doi:10.1002/lno.12536

Hickey, B.M. & Banas, N.S. (2003) Oceanography of the U.S. Pacific Northwest coastal ocean and estuaries with application to coastal ecology. *Estuaries*, **26**, 1010–1031. doi:10.1007/BF02803360

Hiebert, T.C., Thompson, A.W. & Sutherland, K.R. (2025) Diverse microbial prey in the guts of gelatinous grazers revealed by microscopy. *Mar. Biol.*, **172**. doi:10.1007/s00227-025-04615-6

Hill, J.M. & McQuaid, C.D. (2011) Stable isotope methods: The effect of gut contents on isotopic ratios of zooplankton. *Estuar. Coast. Shelf Sci.*, **92**, 480–485, Elsevier Ltd. doi:10.1016/j.ecss.2011.02.002

Huyer, A. & Smith, R.L. (1985) The Signature of El Niño off Oregon, 1982-1983. *J. Geophys. Res.*, **90**, 7133–7142.

Huyer, A. (1983) Coastal upwelling in the California current system. *Prog. Oceanogr.*, **12**, 259–284. doi:10.1016/0079-6611(83)90010-1

Jackson, A.L., Inger, R., Parnell, A.C. & Bearhop, S. (2011) Comparing isotopic niche widths among and within communities: SIBER - Stable Isotope Bayesian Ellipses in R. *J. Anim. Ecol.*, **80**, 595–602. doi:10.1111/j.1365-2656.2011.01806.x

Jacox, M.G., Edwards, C.A., Hazen, E.L. & Bograd, S.J. (2018) Coastal Upwelling Revisited: Ekman, Bakun, and Improved Upwelling Indices for the U.S. West Coast. *J. Geophys. Res. Ocean.*, **123**, 7332–7350. doi:10.1029/2018JC014187

Kelley D, Richards C (2023). _oce: Analysis of Oceanographic Data_. R package version 1.8-2, <https://CRAN.R-project.org/package=oce>.

Kiørboe, T. (2011) How zooplankton feed: Mechanisms, traits and trade-offs. *Biol. Rev.*, **86**, 311–339. doi:10.1111/j.1469-185X.2010.00148.x

Landry, M. R., Postel, J. R., Peterson, W. K., & Newman, J. (1989) Broad-scale distributional patterns of hydrographic variables on the Washington/Oregon shelf. In M. R. Landry & B. M. Hickey (Eds.), *Coastal Oceanography of Washington and Oregon* (1st ed., pp. 1-40). Elsevier Science Publishers B. V. ISBN: 0-444-87308-2

Lerner, J.E., Marchese, C. & Hunt, B.P.V. (2022) Stable isotopes reveal that bottom-up omnivory drives food chain length and trophic position in eutrophic coastal ecosystems. *ICES J. Mar. Sci.*, **79**, 2311–2323. doi:10.1093/icesjms/fsac171

Lesser, J.S., James, W.R., Stallings, C.D., Wilson, R.M. & Nelson, J.A. (2020) Trophic niche size and overlap decreases with increasing ecosystem productivity. *Oikos*, **129**, 1303–1313. doi:10.1111/oik.07026

Lindeman, R.L. (1942) The Trophic-Dynamic Aspect of Ecology. *Ecology*, **23**, 399–417.

Lucas, C.H., Pitt, K.A., Purcell, J.E., Lebrato, M. & Condon, R.H. (2011) What's in a Jellyfish? Proximate and elemental composition and biometric relationships for use in biogeochemical studies. *Ecology*, **92**.

Luo, J.Y., Condon, R.H., Stock, C.A., Lucas, C.H., Pitt, K.A. & Cowen, R.K. (2020) Gelatinous Zooplankton - Mediated Carbon Flows in the Global Oceans : A Data - Driven Modeling Study Global Biogeochemical Cycles. doi:10.1029/2020GB006704

Masterman, J.A., Sutherland, K.R., & Galloway, A.W.E. (2025) Gut Content and Fatty Acid Analyses Reveal Trophic Role of the Ctenophore *Pleurobrachia bachei* in Northern California Current. Manuscript submitted for publication.

Forgrave, K. E., Sweeny, C., Steinman, M., Kerkar, A., Pettit, T., & Thompson, A. W. (2025) Impact of oceanographic gradients and marine heatwaves on the phytoplankton community in the Northern California Current System. Manuscript submitted for publication.

McMahon, K.W., Hamady, L.L. & Thorrold, S.R. (2013) A review of ecogeochemistry approaches to estimating movements of marine animals. *Limnol. Oceanogr.*, **58**, 697–714. doi:10.4319/lo.2013.58.2.0697

Miller, T.W., Brodeur, R.D. & Rau, G.H. (2008) Carbon stable isotopes reveal relative contribution of shelf-slope production to the northern California Current pelagic community. *Limnol. Oceanogr.*, **53**, 1493–1503. doi:10.4319/lo.2008.53.4.1493

Miller, T.W., Brodeur, R.D., Rau, G. & Omori, K. (2010) Prey dominance shapes trophic structure of the northern California Current pelagic food web : evidence from stable isotopes and diet analysis. *Mar. Ecol. Prog. Ser.*, **420**, 15–26. doi:10.3354/meps08876

Mills, C.E. & Goy, J. (1988) In situ observations of the behavior of mesopelagic *Solmissus* narcomedusae (Cnidaria, Hydrozoa). *Bull. Mar. Sci.*, **43**, 739–751.

Minagawa, M. & Wada, E. (1984) Stepwise enrichment of 15N along food chains: Further evidence and the relation between 615N and animal age. *Geochim. Cosmochim. Acta*, **48**, 1135–1140.

Oksanen J, Simpson G, Blanchet F, Kindt R, Legendre P, Minchin P, O'Hara R, Solymos P, Stevens M, Szoecs E, Wagner H, Barbour M, Bedward M, Bolker B, Borcard D, Carvalho G, Chirico M, De Caceres M, Durand S, Evangelista H, FitzJohn R, Friendly M, Furneaux B, Hannigan G, Hill M, Lahti L, McGlinn D, Ouellette M, Ribeiro Cunha E, Smith T, Stier A, Ter Braak C, Weedon J, Borman T (2025). _vegan: Community Ecology Package_. R package version 2.6-10, <https://CRAN.R-project.org/package=vegan>.

Pace, M.L., Cole, J.J., Carpenter, S.R. & Kitchell, J.F. (1999) Trophic cascades revealed in diverse ecosystems. *Trends Ecol. Evol.*, **14**, 483–488. doi:10.1016/S0169-5347(99)01723-1

Pauly, D., Graham, W., Libralato, S., Morissette, L. & Deng Palomares, M.L. (2008) Jellyfish in ecosystems, online databases, and ecosystem models. *Hydrobiologia*, **616**, 67–85. doi:10.1007/s10750-008-9583-x

Peterson, B.J. & Fry, B. (1987) Stable Isotopes in Ecosystem Studies. *Annu. Rev. Ecol. Syst.*, **18**, 293–320.

Peterson, W.T., Miller, C.B. & Hutchinson, A. (1979) Zonation and maintenance of copepod populations in the Oregon upwelling zone. *Deep Sea Res. Part A, Oceanogr. Res. Pap.*, **26**, 467–494. doi:10.1016/0198-0149(79)90091-8

Pitt, K.A., Connolly, R.M. & Meziane, T. (2009) Stable isotope and fatty acid tracers in energy and nutrient studies of jellyfish: A review. *Hydrobiologia*, **616**, 119–132. doi:10.1007/s10750-008-9581-z

Pomerleau, C. & Winkler, G. (2014) The effect of acidification and the combined effects of acidification / lipid extraction on carbon stable isotope ratios for sub-arctic and arctic marine zooplankton species. *Polar Biol.*, **37**, 1541–1548. doi:10.1007/s00300-014-1540-8

Post, D.M., Layman, C.A., Arrington, D.A., Takimoto, G., Quattrochi, J. & Montan, C.G. (2007) Getting to the fat of the matter: models , methods and assumptions for dealing with lipids in stable isotope analyses. *Oecologia*, **152**, 179–189. doi:10.1007/s00442-006-0630-xs1

Post, D.M. (2002) Using stable isotopes to estimate trophic position: Models, methods, and assumptions. *Ecology*, **83**, 703–718. doi:10.1890/0012-9658(2002)083[0703:USITET]2.0.CO;2

Purcell, J.E. & Arai, M.N. (2001) Interactions of pelagic cnidarians and ctenophores with fish: A review. *Hydrobiologia*, **451**, 27–44. doi:10.1023/A:1011883905394

Purcell, J.E. (1982) Feeding and growth of the siphonophore *Muggiaea atlantica*. *Elsevier Biomed. Press*, **62**, 39–54.

Purcell, J.E. (1991) Predation by *Aequorea victoria* on other species of potentially competing pelagic hydrozoans. *Mar. Ecol. Prog. Ser.*, **72**, 255–260. doi:10.3354/meps072255

R Core Team (2023) R: A language and environment for statistical computing. R Foundation for Statistical Computing, Vienna, Austria. URL http://www.R-project.org/

Raskoff, K.A. (2002) Foraging, prey capture, and gut contents of the mesopelagic narcomedusa *Solmissus spp*. (Cnidaria: Hydrozoa). *Mar. Biol.*, **141**, 1099–1107. doi:10.1007/s00227-002-0912-8

Rau, G., Teyssie, J., Rassoulzadegan, F. & Fowler, S. (2021) 13C/12C and 15N/14N variations among size-fractionated marine particles: implications for their origin and trophic relationships. *Mar. Ecol. Prog. Ser.*, **59**, 33–38.

Ryther, J.H. (1969) Photosynthesis and fish production in the sea. *Science (80-.).*, **166**, 72.

Saino T & Hattori A. (1980) 15N natural abundance in oceanic suspended particulate matter. *Nature*, **283**, 752–754.

Schaub, J., McLaskey, A.K., Forster, I. & Hunt, B.P.V. (2021) Experimentally derived estimates of turnover and modification for stable isotopes and fatty acids in scyphozoan jellyfish. *J. Exp. Mar. Bio. Ecol.*, **545**, 151631, Elsevier B.V. doi:10.1016/j.jembe.2021.151631

Schram, J.B., Sorensen, H.L., Brodeur, R.D., Galloway, A.W.E. & Sutherland, K.R. (2020) Abundance, distribution , and feeding ecology of Pyrosoma atlanticum in the Northern California Current. *Mar. Ecol. Prog. Ser.*, **651**, 97–110. doi:10.3354/meps13465

Spitz, Y. H., Allen, J. S., and Gan, J. (2005). Modeling of ecosystem processes on the Oregon shelf during the 2001 summer upwelling. *J. Geophys. Res. Oceans*. **110**, 1–21. doi: 10.1029/2005jc002870

Steinman, M., Schmid, M.S., Cowen, R.K., Sponaugle, S., Sutherland, K.R. & Thompson, A.W. (2024) The microorganisms associated with doliolids in a productive coastal upwelling system. *Limnol. Oceanogr.*, 1–14. doi:10.1002/lno.12748

Stukel, M.R., Selph, K.E., Décima, M., Fender, C.K. & Gutierrez-rodriguez, A. (2024) Gelatinous filter feeders increase ecosystem efficiency. *Commun. Biol.*, **1**, 1–11. doi:10.1038/s42003-024-06717-1

Sumida, B.Y. & Moser, H.G. (1984) Food and feeding of bocaccio (*Sebastes paucispinis*) and comparison with Pacific hake (*Merluccius productus*) larvae in the California current. *Calif. Coop. Ocean. Fish. Investig. Reports*, **25**, 112–118.

Sutherland, K.R. & Thompson, A.W. (2021) Pelagic tunicate grazing on marine microbes revealed by integrative approaches. *Limnol. Oceanogr.*, **67**, 102–121. doi:10.1002/lno.11979

Swanberg, N. (1974) The feeding behavior of *Beroe ovata*. *Mar. Bio.*, **24**, 69-76. doi:10.1007/BF00402849

Wickham, H. ggplot2: Elegant Graphics for Data Analysis. Springer-Verlag New York, 2016.

Wright, R.M., Quéré, C. Le, Buitenhuis, E., Pitois, S. & Gibbons, M.J. (2021) Role of jellyfish in the plankton ecosystem revealed using a global ocean biogeochemical model. *Biogeosciences*, **18**, 1291–1320. doi:10.5194/bg-18-1291-2021

Zhabin, I.A., Vanin, N.S. & Dmitrieva, E.V. (2019) Summer Wind-driven Upwelling and Tidal Mixing on the Western Kamchatka Shelf in the Sea of Okhotsk. *Russ. Meteorol. Hydrol.* **44**, 130–135. doi:10.3103/S1068373919020067